



HAL
open science

Photochemistry of XCH₂CN (X = -Cl, -SH) in Argon Matrices

Joanna Zapala, Thomas Custer, Jean-Claude Guillemin, Marcin Gronowski

► **To cite this version:**

Joanna Zapala, Thomas Custer, Jean-Claude Guillemin, Marcin Gronowski. Photochemistry of XCH₂CN (X = -Cl, -SH) in Argon Matrices. *Journal of Physical Chemistry A*, 2019, 123 (17), pp.3818-3830. 10.1021/acs.jpca.9b01983 . hal-02149782

HAL Id: hal-02149782

<https://univ-rennes.hal.science/hal-02149782>

Submitted on 21 Jun 2019

HAL is a multi-disciplinary open access archive for the deposit and dissemination of scientific research documents, whether they are published or not. The documents may come from teaching and research institutions in France or abroad, or from public or private research centers.

L'archive ouverte pluridisciplinaire **HAL**, est destinée au dépôt et à la diffusion de documents scientifiques de niveau recherche, publiés ou non, émanant des établissements d'enseignement et de recherche français ou étrangers, des laboratoires publics ou privés.

Photochemistry of XCH_2CN ($X=Cl, SH$) in Argon Matrices

Joanna Zapala^a, Thomas Custer^a, Jean-Claude Guillemin^b, Marcin Gronowski^a

^a Institute of Physical Chemistry, Polish Academy of Sciences, Kasprzaka 44/52, PL-01-224
Warsaw, Poland

^b Univ Rennes, Ecole Nationale Supérieure de Chimie de Rennes, CNRS, ISCR – UMR6226, F-
35000 Rennes, France.

*E-mail jzapala@ichf.edu.pl

Abstract

We report infrared spectra and photochemical behavior of the potentially astrochemically significant species, mercaptoacetonitrile ($HS-CH_2C\equiv N$) and, for comparison purposes, chloroacetonitrile ($Cl-CH_2C\equiv N$), both suspended in an argon matrix at 6K. Photolytic formation of the isocyano products $HS-CH_2-NC$ and $Cl-CH_2-NC$ were observed as well as CH_3NSC and CH_3SCN (in $HS-CH_2CN$ photolysis). While no dissociation products were observed for $Cl-CH_2-CN$, photolysis of $HS-CH_2-CN$ produced compounds necessitating the loss of the CN group to form $CH_2=S$, the SH group to form H_2C-CN and $HC-CN$, or both CN and SH to form CH_3 and CH_4 . Observation of emission spectra upon annealing indicates the presence of free sulfur atom in matrices of photolyzed $HS-CH_2-CN$.

1. Introduction

Theoretical studies¹ show that mercaptoacetonitrile ($HS-CH_2-CN$), methyl isothiocyanate (CH_3NCS), and methyl thiocyanate (CH_3SCN) are the three most stable molecules of the C_2H_3NS family having energies of 0, 7.8, and 12.4 kJ/mol respectively. Although not yet detected in the interstellar medium (ISM), each of these can be

1
2
3 considered as a potential candidate. The structurally similar species CH_3SH^2 , $\text{HSCN}^{3,4}$,
4
5 $\text{HNCS}^{3,4}$, and $\text{CH}_3\text{CN}^{5,6}$ have all been detected in the ISM. Hydroxyacetonitrile ($\text{HO-CH}_2\text{-}$
6
7 CN), the closest oxygen-bearing analogue of mercaptoacetonitrile, has been observed in
8
9 laboratory generated interstellar and cometary ice analogs⁷ and recently detected in
10
11 solar-type protostar IRAS16293–2422 B⁸. It is not difficult to imagine replacement of an H
12
13 atom with a CN, NC, or SH group, or addition of a CH_2 or S to one of these known
14
15 astrochemical species to reach the lowest energy members of the $\text{C}_2\text{H}_3\text{NS}$ chemical
16
17 family.
18
19
20

21 While structural analogies are interesting, explicit pathways for formation or
22
23 decomposition of S containing species in space, whether they have already been
24
25 detected or are promising candidates, should be elucidated in the laboratory and through
26
27 calculations. Existing models and the ratio of abundances of different sulfur species have
28
29 already been used to evaluate the age of interstellar clouds^{9,10,11} and to estimate the mass
30
31 of an emerging star¹². However, problems encountered in determination of sulfur
32
33 abundance in the interstellar medium¹³, describing the interstellar synthesis of
34
35 methanethiol (detected in Sagittarius B2 core¹⁴ and hot core of G327.3-0.6¹⁵ but absent
36
37 in TMC-1), and prediction of abundances of nearly all sulfur-containing molecules
38
39 detected in TMC-1^{16,17,9} suggest that our current understanding of sulfur chemistry
40
41 remains incomplete.
42
43
44
45
46
47

48 Here we explore one aspect of sulfur chemistry by describing the computational
49
50 and experimental results of the UV photolysis of mercaptoacetonitrile ($\text{HS-CH}_2\text{-CN}$, MAN)
51
52 and its closely related synthetic precursor chloroacetonitrile ($\text{Cl-CH}_2\text{-CN}$, CAN) in noble
53
54 gas matrices. Although CAN is not of obvious astrochemical significance (Cl abundance
55
56
57
58
59
60

1
2
3 is generally not high in the universe and only a handful of species including AlCl, KCl,
4 NaCl, HCl, HCl⁺, H₂Cl⁺, and CH₃Cl¹⁸ have so far been detected), no noble gas matrix
5
6 photolysis experiments have been performed on this species. As detailed spectroscopic
7
8 information for this molecule is available, photolysis of this chemical provides a
9
10 convenient comparison with mercaptoacetonitrile. While chemically inert noble gas
11
12 matrices are not considered good models for authentic interstellar ices¹⁹, photochemistry
13
14 measurements in this environment can be treated as a first, necessary step toward
15
16 understanding the transformations that might result in a more representative but
17
18 chemically complex ice environment. They also provide a means to produce more exotic
19
20 isomers for spectroscopic characterization. Photochemistry in pertinent interstellar ice
21
22 analogues (e.g., containing CO, H₂O, or other species or mixtures ²⁰) is the next step
23
24 along the path towards understanding photochemical processing in space and will be the
25
26 subject of a future publication.
27
28
29
30
31

32
33 Of the three lowest energy C₂H₃SN family members, mercaptoacetonitrile (HS-
34
35 CH₂-CN), which has a weak chemical stability at room temperature, is the only one not
36
37 commercially available and is therefore less well studied. Nevertheless, this species has
38
39 been explicitly discussed as a likely astrochemical species whose potential routes of
40
41 formation in the interstellar medium were explored and microwave spectrum
42
43 experimentally measured at both -30 °C and room temperature²¹. Synclinal and anti-
44
45 periplanar conformers of mercaptoacetonitrile were identified and their energetic
46
47 separation measured to be 3.8±0.3 kJ/mol. A theoretical study of these two conformers
48
49 has also recently been made in an effort to understand their potential behavior in harsh
50
51 astrophysical environments²². The charge transfer dynamics resulting from collisions
52
53
54
55
56
57
58
59
60

1
2
3 between energetic protons and these isomers was explored and compared to the two
4 lowest-energy HCN dimers (Z and E isomers of cyanomethanimine). Charge transfer of
5 the synclinal conformer turned out to be more efficient than for the corresponding
6 cyanomethanimine.
7
8
9
10

11
12 Outside of these recent works, only a handful of studies on mercaptoacetonitrile
13 are available in the literature. Several synthetic routes to its formation have been explored
14 and routine ^1H and ^{13}C NMR as well as mass spectrometry and IR spectroscopy were
15 used to characterize the products^{23,24,25,26}. Most pertinent to the work at hand are
16 spectroscopic measurements in the infrared and all reported spectra to date are for the
17 pure liquid. Early work of Mathais et al.²³ reported six vibrational bands: the SH group at
18 2560 and 920 cm^{-1} ; the CN group at 2240 cm^{-1} ; and the CH_2 group at 2980, 2940 and
19 1400 cm^{-1} . Wepplo²⁴ gave five unassigned vibrations: 2680, 2260, 990, 925 and 710 cm^{-1} .
20 Gaumont et al.²⁵ reported the SH vibration at 2560 cm^{-1} and CN vibration at 2220 cm^{-1} .
21 Finally, Alexander et al.²⁶ reported a CN vibration at 2247 cm^{-1} . Aside from the vibration
22 at 2680 cm^{-1} ,²⁴ possibly meant to be 2980 cm^{-1} , these comprise a consistent summary of
23 vibrations for this molecule in the liquid phase. They are collected and presented with our
24 results in **Table1 Supporting Information**. No more detailed IR spectral data of
25 mercaptoacetonitrile is available.
26
27
28
29
30
31
32
33
34
35
36
37
38
39
40
41
42
43

44 As for the commercially available chloroacetonitrile ($\text{Cl-CH}_2\text{-CN}$), numerous
45 publications are available and include measurements using a variety of spectroscopic
46 methods. Infrared data was first available in the 1950's, when Zeil et al.²⁷ performed
47 measurements of pure $\text{Cl-CH}_2\text{-CN}$ using IR and Raman spectroscopy and gave a
48 comprehensive list of fundamental vibrations as well as some of their combinations.
49
50
51
52
53
54
55
56
57
58
59
60

1
2
3 Since 50's, various other groups have performed measurements in the gas-phase
4
5 28, 29 or in the liquid-phase 30, 29. Researchers have described the effects of solvation 31,
6
7 28, 32, complexation 33, or change of chlorine substituent 34 on the position of various
8
9 bands. IR band positions 35 and intensities 36 have also been calculated. Nemes et al.³⁷
10
11 estimated absolute intensities for eight vibrations found in the liquid phase and, later the
12
13 same year 38, refined the position of the vibrations and compared their intensities with
14
15 what was measured in the gas phase as well as in carbon disulfide (CS₂). Thomas et al.³⁹
16
17 investigated the CN stretching band in more detail and estimated its absolute intensity,
18
19 focusing on the effect of environment and phase change on its intensity. Finally, George
20
21 et al.⁴⁰ reported hydrogen chloride mode of Cl-CH₂-CN:HCl complex at 2709 cm⁻¹ in an
22
23 Ar matrix at 7K although no band positions for the matrix isolated Cl-CH₂-CN species
24
25 alone were given. The positions and intensities of Cl-CH₂-CN vibrations published by
26
27 abovementioned authors are collected in **Table2 Supporting Information**.
28
29
30
31
32

33 While the photochemistry of both HS-CH₂-CN and Cl-CH₂-CN species has not
34
35 been described, a rich literature concerning transformations of small molecules is
36
37 available to suggest potential processes that might occur upon UV irradiation. Due to the
38
39 matrix cage effect 41, 42 loss of larger moieties (e.g., fragments such as CN or CH₃) following
40
41 bond breakage is generally not observed and isomerization is the most probable process.
42
43 Nevertheless some fraction of these fragments may escape. Depending on the energy
44
45 available and rare gas used, H, Cl or S atoms can end up being separated to leave
46
47 radicals, ions, or other isomeric combinations.
48
49
50

51 Concerning isomerization of cyano species, UV irradiation of cyanoacetylene
52
53 (HC₃N) trapped in noble gas matrix leads to the formation of several isomers of the parent
54
55
56
57
58
59
60

1
2
3 molecule, including isocyanoacetylene (HCCNC) and an imine (HNC₃)⁴³. Both of these
4
5 isomers have been already detected in the interstellar medium accompanying the more
6
7 abundant cyanoacetylene. Kawaguchi et al. identified HCCNC⁴⁴ and later the same year
8
9 HNCCC⁴⁵ in Taurus Molecular Cloud 1 (TMC-1). Gensheimer et al.⁴⁶ identified both
10
11 isomers in IRC +10216 and Vastel et al. in the L1544 pre-stellar core⁴⁷. The formation of
12
13 isocyanides from cyano precursors in a matrix environment has been observed for a
14
15 variety of unsaturated cyanoacetylenes including HC₃N, HC₅N⁴⁸, NC₄N⁴⁹, NC₆N⁵⁰, and
16
17 C₂H₃CN⁵¹ among others. Nevertheless, it is not a foregone conclusion that such
18
19 cyano/isocyano rearrangement must occur for any arbitrary cyanide containing species.
20
21
22

23
24 Photolysis of thiol species of the form R-SH results mainly in scission of C-S and
25
26 S-H bonds^{52,53,54} with the main products being radicals and, depending on photolysis
27
28 conditions, various radical recombination products. In 195 nm flash photolysis
29
30 experiments on gaseous CH₃SH Callear et al.⁵² observed formation of CH₃S, CH₃ and
31
32 other radicals using UV absorption spectroscopy while 254nm photolysis of C₂H₅SH in a
33
34 xenon matrix was shown to produce the thiyl radical C₂H₅S*⁵⁵. Photolysis of CH₃SH vapor
35
36 in 254 and 214 nm has been shown to produce H₂, H₂S, C₂H₄, C₂H₆ and CH₃SSCH₃⁵³;
37
38 C₂H₅SH vapor photolysed in the same conditions produced H₂, H₂S, C₂H₄, C₂H₆⁵⁶ and
39
40 C₂H₅SSC₂H₅⁵⁷.
41
42
43

44
45 Hydrogen atom production and escape of H₂ from the matrix cage has been
46
47 reported as well, producing even more complex, dehydrogenated species, where
48
49 photolysis of methanethiol at 121nm in a nitrogen matrix at 14 K leads to formation of
50
51 CH₄, CS, CS₂, CH₃ and H₂CS as the main products⁵⁸.
52
53

54
55 Lastly, studies of photolysis of alkyl halides in matrixes^{59, 60} show that the cage
56
57
58
59
60

1
2
3 effect can inhibit halogen detachment processes. Photolysis of methyl chloride CH_3Cl in
4
5 Ar and N_2 matrixes⁶⁰ was found to yield CCl , HCCl and H_2CCl as major products in
6
7 addition to smaller amounts of CH_3 , HCl and CH_4 .
8
9

10 Based on these works, the most likely result of mercaptoacetonitrile or
11
12 chloroacetonitrile photolysis should involve CN/NC isomerization or be products of $-\text{H}$ or
13
14 $-\text{SH}$ elimination.
15
16
17
18

19 2. Theoretical methods

20
21
22
23

24 A combination of two methods of solving the electronic Schrödinger equation was used
25
26 for these studies to arrive at vibrational frequencies. Density functional theory with the 3-
27
28 term correlation functional of Becke⁶¹ and the exchange functional of Lee, Yang, and
29
30 Parr⁶² (B3LYP) were used with vibrational second-order perturbation theory^{63,64,65,66} to
31
32 calculate anharmonic frequencies and intensities. The *ab initio* coupled cluster method,
33
34 truncated to iterative treatment of single and double excitations and the perturbative
35
36 treatment of triple excitations (CCSD(T))^{66,67,68,69,70,71} were used during computation of
37
38 harmonic frequencies. The triple- ζ Dunning-type basis set (cc-pVTZ)⁷² was chosen for
39
40 the CCSD(T) calculations while its augmented version (aug-cc-pVTZ)⁷³ was used for
41
42 B3LYP computations. All vibrational calculations were preceded by geometry
43
44 optimization at the same level of electronic structure theory and the Gaussian 09⁷⁴
45
46 program was used for all computations. Vibrational frequencies ultimately reported were
47
48 calculated using the following equation:
49
50
51
52

$$53 \nu_{rec} = \omega_{CCSD(T)} + (\nu_{B3LYP} - \omega_{B3LYP}); \quad (1)$$

54
55
56
57
58
59
60

1
2
3 where $\omega_{CCSD(T)}$ and ω_{B3LYP} are harmonic frequencies computed either using CCSD(T) or
4 B3LYP methods and ν_{B3LYP} is the anharmonic frequency computed using B3LYP as
5 described previously. This methodology has been successfully applied in earlier studies
6
7
8
9
10 ⁷⁵⁻⁷⁷ and in other systems where the resulting vibrational frequencies generally had an
11
12 accuracy better than 10 cm⁻¹ ⁷⁸.
13
14
15
16

17 3. Experimental methods 18 19 20

21 The HS-CH₂-CN used in these experiments was synthesized according to Gaumont
22 et al.²⁵, purified as reported by Møllendal et al.²¹ and stored either with or without
23 Amberlyst at -80°C. This malodorous compound decomposes vigorously at room
24 temperature or under basic conditions. The kinetic stability of this compound is strongly
25 dependent on the temperature and the presence of acidic compounds. Although
26 Amberlyst may stabilize the chemical for long-term storage, it also proved to be a strong
27 source of methanol which was trapped in its pore spaces during previous synthetic steps.
28 The chemical proved to be sufficiently stable without Amberlyst for use in these photolysis
29 experiments.
30
31
32
33
34
35
36
37
38
39
40
41

42 Chloroacetonitrile, Cl-CH₂-CN was purchased (98%, abcr GmbH).
43

44 Spectroscopic measurements were performed on a Bruker Vertex 70 instrument
45 equipped with a KBr beam splitter and liquid-nitrogen-cooled MCT (HgCdTe) detector in
46 the 400-6000 cm⁻¹ spectral range at the maximum available resolution of 0.16 cm⁻¹.
47 Degassed HS-CH₂-CN or Cl-CH₂-CN was combined with Ar (5.0 Multax s.c.) at a ratio of
48
49
50
51
52
53
54
55
56
57
58
59
60 1:1000 in a stainless steel vacuum manifold with partial pressures measured using

1
2
3 capacitance manometers (10 torr and 1000 torr, MKS instruments). Following two hours
4
5 to allow for mixing of HS-CH₂-CN or Cl-CH₂-CN with Ar in the manifold, samples were
6
7 deposited onto a CsI window pre-cooled to 5-6 K inside a vacuum chamber (~10⁻⁷ Torr).
8
9 Cooling was accomplished using a closed-cycle helium refrigerator (DE-202SE Advanced
10
11 Research Systems) whose temperature was controlled using a LakeShore 325
12
13 temperature controller. The cold window was positioned at 45° with respect to the path of
14
15 IR radiation of the spectrometer and deposition was carried out at a flow rate of ca. 0.1
16
17 mmol/minute through a capillary nozzle of 1 mm diameter terminating ~2cm from the cold
18
19 window. The total amount of the mixture deposited never exceeded 8 mmol (~300 Torr).
20
21
22
23

24 Lower limits of absolute intensities were calculated using the formula from ⁷⁹, by
25
26 Szczepaniak et al.: $A\left[\frac{km}{mole}\right] = \frac{2.3031}{100 * c * D} \int \log \frac{I_0}{I} dv$. In this expression, c is the molar
27
28 concentration of HS-CH₂-CN or Cl-CH₂-CN in $\left[\frac{mmole}{cm^3}\right]$, D is the film thickness [cm], $\log \frac{I_0}{I}$ is
29
30 the measured absorbance of the band, and ν is the wavenumber [cm^{-1}]. The molar
31
32 concentration was calculated using $c = \frac{p(\text{HSCH}_2\text{CN or ClCH}_2\text{CN})}{p(\text{argon})} \cdot \rho$ where ρ is the density of solid
33
34 argon with a value of $44 \frac{mmole}{cm^3}$ ⁷⁹ and p is the measured partial pressure of the pertinent
35
36 species. It is assumed that both the chemical and the rare gas are sufficiently pure that
37
38 the partial pressures measured are not affected by any other species and that this ratio
39
40 is conserved through deposition and in the ice itself. Observed bands were integrated
41
42 using the OPUS program (Bruker Optik GmbH 2014). The thicknesses of the deposited
43
44 matrices were determined by monitoring reflected He-Ne laser light⁸⁰ as well as using
45
46 interference fringes observable in IR spectra. For the laser thickness measurements, a
47
48 fixed-frequency He-Ne laser (ThorLabs HNL050R model, $\lambda = 632.5$ nm) was directed
49
50
51
52
53
54
55
56
57
58
59
60

1
2
3 towards a growing matrix. Interference was produced in the laser light reflected by the
4 vacuum-ice and ice-substrate interfaces which have different and changing optical paths
5 as film growth proceeds. Reflected light intensity as a function of time was recorded using
6 a portable CCD spectrometer equipped with a fiber optic that could be adjusted outside
7 of the vacuum chamber to capture the reflected laser light (Mightex CCD, HRS series).
8 The intensity of the reflected laser light oscillates between periods of constructive and
9 destructive interference as a function of time. While the time of one oscillatory period is a
10 function of deposition rate, the change in thickness produced over the course of one
11 period is constant. Because of this, the total thickness of a matrix can be estimated by
12 counting the number of fringes starting from time zero until deposition is stopped (or an
13 arbitrary time of interest) and using the following relationship presented by Urso et al.⁸⁰:

$$24 \quad D = m\Delta d = \frac{m\lambda_0}{2n_f\sqrt{1 - \sin^2\theta_i/n_f^2}} .$$

25 In this equation, D is the film thickness (total thickness of the

26 matrix) [cm], m is the number of fringes observed, Δd is the thickness increase between
27 two fringes [cm], θ_i is incidence angle of the laser with respect to the cold target, n_f is the
28 refractive index of the film, and λ_0 is the wavelength of laser light: 6.325×10^{-5} [cm]. We
29 assumed n_f to be similar to pure argon for our experimental conditions, a reasonable
30 assumption given the 1:1000 ratio of chemical to Ar. A refractive index value of 1.52 was
31 used for solid Ar at 6 K⁸¹. Thickness information can also be retrieved from IR spectra
32 directly using interference fringes which, in a well ordered ice, manifest as an undulating
33 baseline in our spectra. In this method, a modified equation was used ⁸⁰:

$$34 \quad D = \frac{1}{l * 2n_f \sqrt{1 - \frac{\sin^2\theta_i}{n_f^2}}}$$

35 , where D is the film thickness [cm], l is the distance between the fringes [cm⁻¹], θ_i is
36 incidence angle of the IR light with respect to the cold target, and n_f is the refractive index
37
38
39
40
41
42
43
44
45
46
47
48
49
50
51
52
53
54
55
56
57
58
59
60

1
2
3 of the film. The equivalence of these two methods of thickness determination was verified
4
5 for pure Ar matrices by depositing a measured amount of noble gas while monitoring
6
7 using laser interference fringes. At specified points, deposition was interrupted (0.625
8
9 mmol, 1.25 mmol, 2.5 mmol, 3.75 mmol, and 5 mmol) so IR spectral fringes could be
10
11 measured. Good agreement between both methods was obtained with a difference of
12
13 approximately 10%. In another series of experiments, thickness estimated from the
14
15 pattern in our IR spectra was measured as a function of incident angle θ_i and gave an
16
17 error typically less than 2%.
18
19
20

21
22 Both HS-CH₂-CN and Cl-CH₂-CN were exposed to UV irradiation generated by an
23
24 excimer laser. HS-CH₂-CN samples were irradiated either using at 248 nm (KrF excimer)
25
26 for 2.5 hours or 193 nm (ArF excimer) for 1.5-2.5 hours with an average laser pulse
27
28 frequency of 10 Hz and power of 1 mJ per pulse (approx. 0.2 mJ/cm³) measured just in
29
30 front of the quartz window of the vacuum chamber using a pyroelectric sensor (Ophir
31
32 Optronics PE50B). Cl-CH₂-CN was irradiated at 193 nm (ArF excimer) for 2 hours with
33
34 an average laser pulse frequency of 10 Hz and power of 0.5 mJ per pulse (approx. 0.1
35
36 mJ/cm³). Annealing was performed as the last step of sample processing and consisted
37
38 of raising the temperature of the sample to ~35 K for a period of 20 min and then re-
39
40 cooling to the original value. Emission observed during annealing was recorded using a
41
42 Mightex CCD spectrometer (HRS series, 300-1070 nm spectral range, 1.7 nm resolution).
43
44 IR spectra taken following annealing were used to confirm that various groups of product
45
46 signals belonged to the same species (either increasing or decreasing together).
47
48
49
50
51
52
53
54
55
56
57
58
59
60

4. Results

4.1 Theory

Theoretical IR frequencies, intensities, and rotational constants for mercaptoacetonitrile (HS-CH₂-CN) along with other C₂H₃SN isomers have been published previously¹. Only a comparison of predicted anharmonic IR frequencies for synclinal and anti-periplanar conformers, not provided in the previous work, are given here in **Table 1**. Similar calculations to those performed for C₂H₃SN isomers were also performed for the C₂H₂NCl family of isomers which includes Cl-CH₂-CN (CAN). First, B3LYP/aug-cc-pVTZ computations were used to estimate relative energies for different isomers of the C₂H₂NCl family (**Fig 1**) starting from structures for which Lewis dot diagrams could be drawn as closed shell molecules. Both singlet and triplet states were optimized for each structure. More precise computations at the CCSD(T)/cc-pVTZ level were then performed for CAN, CAN-1, and CAN-2. The relative energies are collated in **Fig 1** and vibrational frequencies in **Tables 2A, 2B, and 2C**. Although CAN isomers are not likely candidates for detection in space, the microwave spectrum of CAN has already been reported and the rotational constants and dipole moments for the three lowest energy isomers of CAN given in **Table 3** may prove useful for an eventual radioastronomical search or microwave measurements. In this table, ground state rotational constants are calculated at the CCSD(T)/cc-pVTZ level of theory and differences between ground state and equilibrium rotational constants at B3LYP/aug-cc-pVTZ. Without including core electron correlation and approaching the complete basis set limit, the precision of these rotational constants is likely a little more than 1%, a limitation that will be addressed in a future publication.

The predicted dipole moments for these molecules are high, which suggests that their detection during any eventual experimental rotational spectroscopy studies should be facile.

Fig 1 Structures of isomers of C_2H_2ClN stoichiometry. The B3LYP relative energies are given for all isomers, while CCSD(T) (bold in parenthesis) relative energies are given only for the three lowest energy isomers.

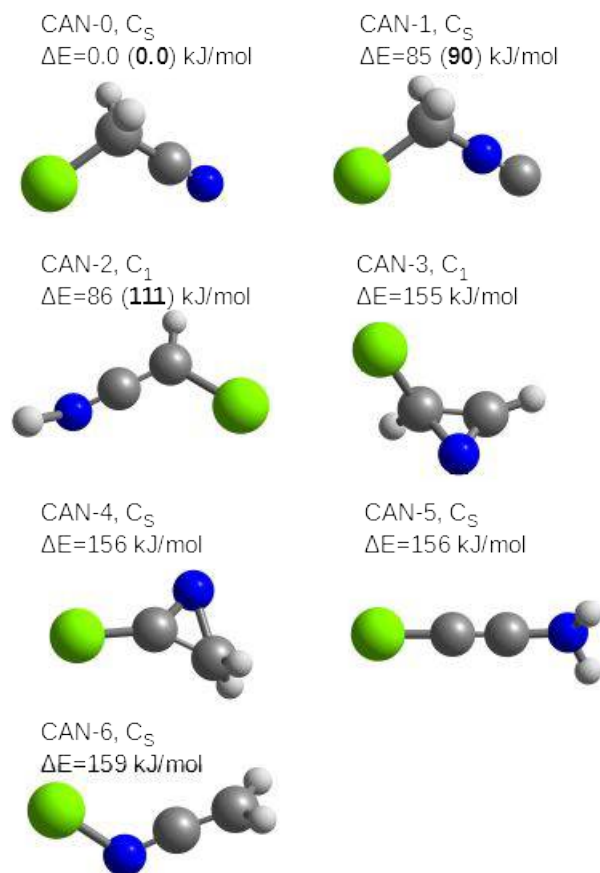


Table 1 Comparison of predicted frequencies and intensities for two conformers of HS-CH₂-CN (MAN) along with experimental values measured in an Ar matrix.

Mode ^{g)}	Freq. [cm ⁻¹]			Inten. [km mol ⁻¹] (Rel. Int. [unitless])		
	Anti-periplanar ^{a)}	Synclinal ^{a) c)}		Anti-periplanar ^{b)}	Synclinal ^{b)}	
	Calc.	Calc.	Exp.	Calc.	Calc.	Exp. ^{h)}
v ₁	2987	2988 (2994)	3014	0	1 (17)	2.0 (5)
v ₂	2965	2964 (2979)	2951	2	3 (50)	1.3 (22)
v ₃	2530	2582 (2604)	2607	1	0 (0)	0.5 (9)
v ₄	2261	2256 (2274)	2256	5	6 (100)	1.5 (26)
v ₅	1434	1426 (1435)	1419 ^{d)}	4	6 (100)	6.3 (100)
v ₆	1241	1254 (1258)	1249.7 ^{d)}	14	5 (83)	3.0 (45)
v ₇	1167	1195 (1200)	1193	1	2 (33)	0.8 (13)
v ₈	972	998 (956)	997	1	3 (50)	4.0 (67)
v ₉	878	921 (931)	926	1	5 (83)	7.0 (92)
v ₁₀	845	793 (788)	786	2	1 (17)	0.7 (11)
v ₁₁	709	694 (704)	701	1	5 (83)	3.7 (63)
v ₁₂	461	475 (484)	-	2	0	-
v ₁₃	346	351 (364)	e)	1	0	-
v ₁₄	165	273 (203)	e)	3	37	-
v ₁₅	247	193 (171)	e)	7	21	-

a) combined CCSD(T)/anharmonic B3LYP calculation, see equation (1)

b) anharmonic B3LYP

c) in parentheses, results of anharmonic CCSD(T) computations¹

d) two sites were observed with the most intense reported in the table (**Fig.1**)

e) out of detection range

f) Relative intensities given with respect to v₅ located at 1419 cm⁻¹ (experimental) rather than the most intense mode which is outside of our measurement range.

g) None of the computed overtones has an intensity higher than 1 km mol⁻¹ and are not reported

h) lower limit of absolute intensity

Table 2A Comparison of predicted frequencies and intensities of Cl-CH₂-CN (CAN) along with experimental values measured in an Ar matrix.

Mode f)	Symmetry	Freq. [cm ⁻¹]		Freq. shift ³⁵ Cl→ ³⁷ Cl [cm ⁻¹]		Int. [km mol ⁻¹] (Rel. Int. [unitless])	
		Calc. ^{a)}	Exp.	Calc. ^{b)}	Exp.	Calc. ^{c)}	Exp. ^{g)}
v ₁	A'	2990	2972.1	0		4 (12)	2.3 (8)
v ₂	A'	2259	2263.4	0		0 (0)	0.6 (2)
v ₃	A'	1437	1431.1	0		5 (15)	5.1 (18)
v ₄	A'	1268	1271.1	0		18 (53)	9.3 (33)
v ₅	A'	929	930.8	0		15 (44)	24.9 (89)
v ₆	A'	750	745.4	-4	-4	34 (100)	28.0 (100)
v ₇	A'	476	484.2	-3	-3.5	5 (15)	2.1 (7)
v ₈	A'	181	^{d)}	-1		6 (17)	-
v ₉	A''	3020	3014.3	0		0 (0)	3.1 (11)
v ₁₀	A''	1183	1183.4	0		0 (0)	0.4 (1)
v ₁₁	A''	908	906.7	0		1 (0)	0.9 (3)
v ₁₂	A''	336	^{d)}	0		1 (0)	-

a) combined CCSD(T)/anharmonic B3LYP calculation, see equation (1)

b) harmonic CCSD(T)

c) anharmonic B3LYP

d) out of detection range

e) relative intensities with respect to v₆ at 745 cm⁻¹

f) None of the computed overtones has an intensity higher than 1 km mol⁻¹ and are not reported.

g) lower limit of the absolute intensities

Table 2B Comparison of predicted infrared frequencies and intensities of Cl-CH₂-NC, CAN-1 along with experimental values measured in an Ar matrix.

Mode		Freq. [cm ⁻¹]		Freq. shift ³⁵ Cl→ ³⁷ Cl [cm ⁻¹]		Rel. Int. [unitless]	
		Calc. ^{a)}	Exp.	Calc. ^{b)}	Exp.	Calc. ^{c)}	Exp. ^{e)}
v ₁	A'	3002	3035.9	0		4	19
v ₂	A'	2137	2143.8	0		100	100
v ₃	A'	1457	1453.0	0		2	1
v ₄	A'	1311	1306.2	0		24	12
v ₅	A'	962	962.3	0		30	19
v ₆	A'	746	777.4	-4	-1.2	43	87
v ₇	A'	418	477.7	-3	-1.4	1	23
v ₈	A'	160	^{d)}	-1		2	-
v ₉	A''	3032	3036.0	0		0	19
v ₁₀	A''	1229	1228.2	0		1	1
v ₁₁	A''	951	-	0		0	-
v ₁₂	A''	242	^{d)}	0		0	-
Combination modes and overtones with intensities higher than 1 km × mol ⁻¹							
2v ₅		1908	-	0		1	-
v ₅ +v ₄		2271	-	0		1	-
v ₆ +v ₃		2202	2208.0	-5		6	1
v ₈ +v ₂		2293	-	-1		1	-
v ₈ +v ₄		1114	-	-1		1	-
v ₉ +v ₃		4467	-	0		1	-
v ₁₁ +v ₁₀		2180	2179.0	0		30	1
v ₁₂ +v ₂		2370	-	0		1	-

a) combined CCSD(T)/anharmonic B3LYP calculation, see equation (1)

b) harmonic CCSD(T)

c) anharmonic B3LYP, relative intensities with respect to v₂ (178 km/mol)

d) out of detection range

e) relative intensities given with respect to v₂

Table 2C Predicted infrared frequencies and intensities of HNCCHCl, CAN-2

Mode	Freq. [cm ⁻¹] ^{a)}	Freq. shift ³⁵ Cl→ ³⁷ Cl [cm ⁻¹] ^{b)}	Inten. [km mol ⁻¹]
v ₁	3281	0	15
v ₂	3114	0	18
v ₃	2047	0	227
v ₄	1290	0	40
v ₅	1125	0	9
v ₆	1019	0	186
v ₇	837	0	67
v ₈	781	-4	34
v ₉	536	-1	39
v ₁₀	532	-3	2
v ₁₁	409	0	26
v ₁₂	182	-1	0
Combination modes and overtones with intensities higher than 1 km × mol ⁻¹			
v ₁	6389	0	13
v ₂	6112	0	1
v ₃	4067	0	3
v ₆	2005	0	35
v ₈	1559	-7	1
v ₉	1078	-1	1
v ₁₀	1059	-6	5
v ₄ +v ₃	3321	0	3
v ₆ +v ₃	3071	0	2
v ₆ +v ₄	2311	0	2
v ₆ +v ₅	2145	0	8
v ₉ +v ₇	1371	-1	7
v ₁₀ +v ₉	1067	-4	1
v ₁₁ +v ₆	1436	0	1
v ₁₁ +v ₇	1249	0	1
v ₁₁ +v ₉	943	-1	14
v ₁₁ +v ₁₀	941	-3	2

a) combined CCSD(T)/anharmonic B3LYP calculation, see equation (1)

b) harmonic CCSD(T)

c) anharmonic B3LYP results

Table 3 Rotational constants and dipole moment for selected isomers of CAN

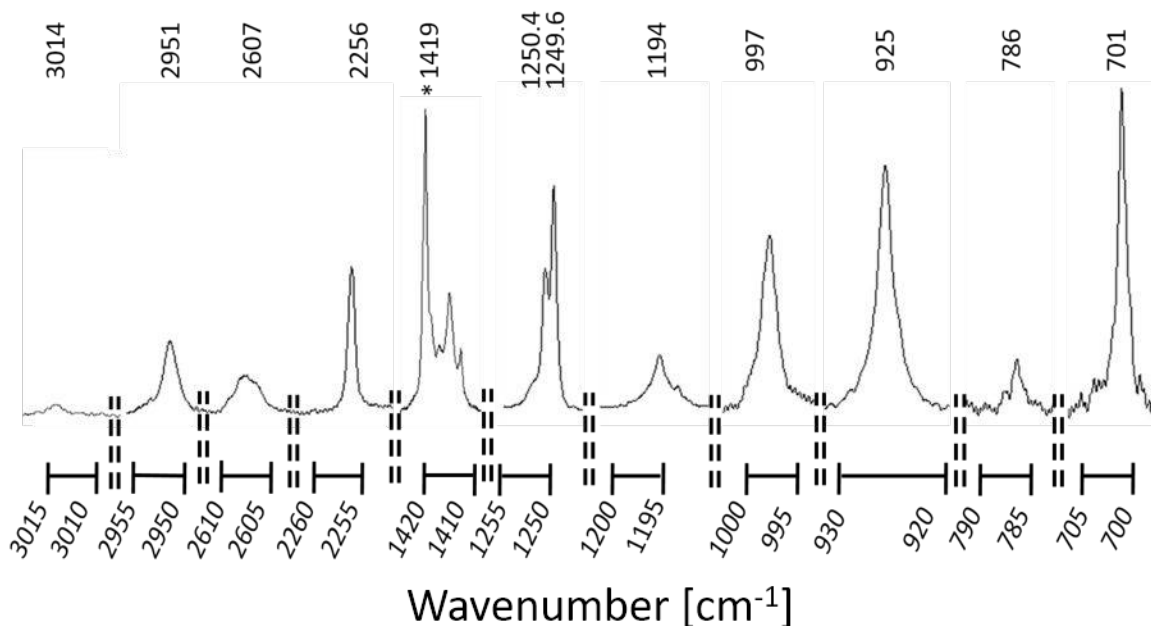
	A_0/MHz	B_0/MHz	C_0/MHz	μ_e/D
CAN	25045	3109	2811	3.28
	25271.3583(45) ^{a)}	3150.74897(102) ^{a)}	2789.4927(22) ^{a)}	
CAN-1	25758	3327	2999	3.04
CAN-2	34114	2919	2705	1.89

a) ground state experimental values ⁸²

4.2 Spectroscopy

Prior to photolysis, the spectrum of pure HS-CH₂-CN in a noble gas matrix was recorded (**Fig. 2**) and analyzed. The measured IR band positions along with lower limits for absolute and relative intensities are presented in **Table 1** along with theoretically predicted values for synclinal and anti-periplanar forms (for structures of synclinal and anti-periplanar forms, see **Figure 1** from ⁸³).

Fig2 Experimental IR spectra of HS-CH₂-CN for pertinent regions of **Table 1**. Y scale is the intensity in arbitrary units.



* all regions share a common y-scale except for the feature at 1419 cm⁻¹ which has been reduced by a factor of 2.

1
2
3 Since HS-CH₂-CN is not a particularly rigid molecule, containing only a single, non-
4 conjugated multiple bond, it might be expected to exhibit interesting site structures upon
5 trapping in solid Ar or broadening due to allowed molecular motions within a matrix cage.
6 However, IR absorption bands were narrow and only the peaks located near 1250 cm⁻¹
7 and 1419 cm⁻¹ had easily discernable structure. For the doublet near 1250 cm⁻¹, a typical
8 ratio between components of 3:2 was observed with the higher intensity signal at 1249.6
9 cm⁻¹.
10
11
12
13
14
15
16
17
18

19 The absolute value of the difference between measured and predicted frequencies
20 of the synclinal conformer ranges between 0 and 26 cm⁻¹. The sign of the difference
21 depends on the band being considered. Overall, these deviations are generally 1% or
22 less of the experimentally measured frequency. In light of considerable differences
23 between HS-CH₂-CN as a pure liquid and in an Ar matrix environment, our matrix
24 measurements are also remarkably consistent with reports for the pure liquid in the
25 literature and reveal additional vibrations at 786, 1193, 1249.7, 1250.4, and 2607 cm⁻¹
26 which have not yet been described (**Table 1 Supporting Information**).
27
28
29
30
31
32
33
34
35
36
37

38 Relative intensities were determined over the course of six experiments. Deviation
39 of intensities for each vibration ranged between 4.9% and 10.6% (6.6% on average) for
40 ten out of 11 bands. The highest frequency vibration (for which RSD was 30%) was
41 excluded from this analysis as its very low intensity hindered proper peak integration.
42 Absolute intensities measured for HS-CH₂-CN were consistently smaller than values
43 predicted by calculations by a factor of 5 in five out of six experiments conducted. These
44 errors are larger than would be expected based on determination of matrix thickness or
45 peak integration for which the error should be around 9-11%. As these six experiments
46
47
48
49
50
51
52
53
54
55
56
57
58
59
60

1
2
3 were conducted using two different synthetic batches of the chemical (one experiment
4 with the first batch and the five subsequent experiments with the second), this
5 discrepancy is most likely due to partial decomposition of the second batch of HS-CH₂-
6 CN during the vaporization and deposition. Work with this highly reactive compound was
7 difficult. For this reason, we present the higher values obtained from the single experiment
8 in **Table 1** that more closely match theoretical predictions. For this specific determination,
9 measured absolute intensities vary from predicted values by factors between 0.5 and 4
10 depending on the band considered. The same goes for relative intensities which varied
11 from predictions by factors between 0.7 and 3.8. Although this variation is significant, the
12 pattern of intensities of the various bands qualitatively resembles one another when
13 comparing experiment to theory.
14
15
16
17
18
19
20
21
22
23
24
25
26
27

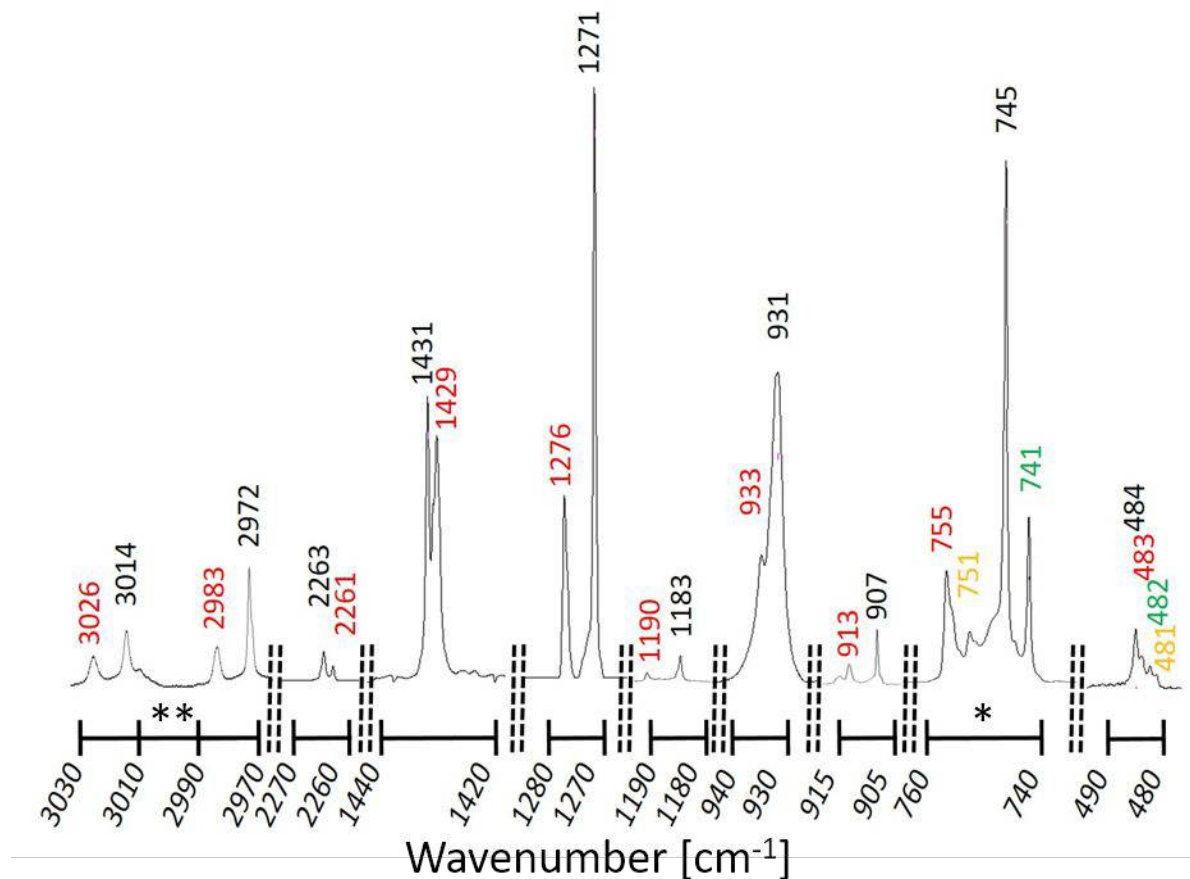
28
29
30
31
32
33
34
35
36
37
38
39
40
41
42
43
44
45
46
47
48
49
50
51
52
53
54
55
56
57
58
59
60

Microwave studies indicate that HS-CH₂-CN can exist in either anti-periplanar or
synclinal configurations in the gas phase at room temperature ⁸³ and that these forms
have an energy difference of 3.8±0.3 kJ/mol. Studies of L-isoserine ⁸⁴ and β-alanine ⁸⁵
indicate that it is sometimes possible to conserve ratios between conformers during matrix
deposition. Based on the computed differences in vibrational frequencies of anti-
periplanar and synclinal forms of HS-CH₂-CN (**Table 1**), the resolution of our
spectrometer and observed peak widths, these conformers should be easily
distinguishable in these measurements should they both become frozen in the Ar ice. The
computed (CCSD(T)/cc-pVTZ) energetic difference between conformers is 4.5 kJ/mol,
close to the experimental value, and indicate a 4.1 kJ/mol difference between conformer
free enthalpies at room temperature. Assuming thermal equilibrium between isomers, a
ratio of ~5:1 (synclinal to anti-periplanar) should be observed. However, no obvious sign

1
2
3 of their coexistence could be found in the measured spectra. Measured IR frequencies
4 are in better agreement with what is predicted for the synclinal form, the more stable of
5 the two conformations. As the absolute intensities are low for both compounds and IR
6 signals from the most stable isomer were already small, it may be that we were simply
7 unable to detect bands of the less abundant anti-periplanar conformer.
8
9

10
11
12
13
14 The Cl-CH₂-CN purchased for these experiments had excellent purity and
15 identification of peaks was unambiguous based on previous reports. Comparison
16 between calculated and experimentally determined values of intensities and position of
17 peaks of Cl-CH₂-CN are presented in **Table 2A**. The experimental IR spectrum of Cl-CH₂-
18 CN is presented in **Fig 3**. Most peaks appear as overlapping doublets suggesting
19 existence of at least two different matrix sites. In **Table 2A**, the more intense member of
20 the doublet is reported. For the ν_6 and ν_7 vibrations a quartet is observable. For ν_6 , peaks
21 at 745 and 755 cm⁻¹ are assigned to the two matrix sites of ³⁵Cl-CH₂-CN and the less
22 intense peaks at 741 and 751 cm⁻¹ were attributed to matrix sites of the ³⁷Cl-CH₂-CN
23 isomer. For ν_7 , more intense features at 484 and 483 cm⁻¹ were again assigned to ³⁵Cl-
24 CH₂-CN and the smaller 482 and 481 cm⁻¹ bands to ³⁷Cl-CH₂-CN.
25
26
27
28
29
30
31
32
33
34
35
36
37
38
39
40
41
42
43
44
45
46
47
48
49
50
51
52
53
54
55
56
57
58
59
60

Fig3 Experimental IR spectra of $\text{Cl-CH}_2\text{-CN}$ (see **Table 2A**). Y scale is the intensity in arbitrary units.



Matrix sites assigned to $^{35}\text{Cl-CH}_2\text{-CN}$ (black and red) and matrix sites for $^{37}\text{Cl-CH}_2\text{-CN}$ (green and yellow). * all regions share a common y-scale except for the region between 740 cm^{-1} and 760 cm^{-1} which was reduced by a factor of 2. **all regions share the same x scale except for the region between 3030 cm^{-1} and 3010 cm^{-1} which was reduced by a factor of 2

Comparing theoretically predicted values of IR absorption frequencies to experimentally observed values, differences range between 0.4 and 18 cm^{-1} with the sign of the deviation varying depending on the mode being considered. This amounts to less than 1% of the measured value for all modes except for that for ν_7 at 476 cm^{-1} which differs by $\sim 1.7\%$. The position of vibrations was also very similar to previously reported in liquid and in gas phase and ranges between 0 and 14 cm^{-1} (**Table 2 Supporting**

1
2
3 **Information**). We were not able to detect any of the overtones or combinations reported
4
5 in the work of Zeil et al.²⁷. Our inability to observe such features is consistent with our
6
7 calculations which indicate they should have very low intensities. While no new features
8
9 of this molecule were detected in our study, no author has reported vibrations from ³⁷Cl-
10
11 CH₂-CN isotopomer or peak locations in a noble gas matrix.
12
13

14
15 Measured absolute intensities are again smaller than theoretical predictions,
16
17 although they are much closer than those measured for HS-CH₂-CN. Measured values
18
19 are only smaller than theoretical values by up to a factor of around 2.4 depending on the
20
21 band being considered. Better agreement likely has to do with the higher purity and
22
23 stability of the commercially available chemical.
24
25

26
27 Absolute intensities have been measured previously in the liquid phase by Nemes
28
29 et al.³⁸ and by Thomas et al.³⁹ for the CN vibration. They are several times larger than
30
31 both our experimental and calculated values. Absolute intensities were also calculated by
32
33 Wladkowski et al.³⁶. Despite their moderate level of theory, their values are quite similar
34
35 to our own.
36
37
38
39

40 4.3 Photochemistry

41
42
43

44
45 HS-CH₂-CN was irradiated using either 248 or 193 nm laser light and the results
46
47 of photolyses at these wavelengths are given in **Table 4** and include photoproduct peak
48
49 positions, intensities, behavior upon annealing, and assignments. Arrows in the anneal
50
51 column indicate whether the intensity of a given peak in the IR spectrum increased (up)
52
53 or decreased (down) following annealing. Intensity values are given relative to the highest
54
55
56
57
58
59
60

1
2
3 intensity photoproduct peak (a value of 100) to provide information about ease of
4
5 detection of various products as well as peak ratios for bands assigned to the same
6
7 photoproduct. Values of intensities are based on their integrals.
8
9
10
11
12
13
14
15
16
17
18
19
20
21
22
23
24
25
26
27
28
29
30
31
32
33
34
35
36
37
38
39
40
41
42
43
44
45
46
47
48
49
50
51
52
53
54
55
56
57
58
59
60

Table 4 Peaks observed after HS-CH₂-CN laser photolysis.

Freq. [cm ⁻¹]	anneal	Rel. Int. ^{a)} [unitless] photolysis 248 nm	Rel. Int. ^{a)} [unitless] photolysis 193 nm	Assignment
3611	↓	32	9	
3233	↓	47	-	HC-CN
3219	↓	29	69	
3162	↓	-	100	
2168	↓	3	2	CH ₃ SCN
2142	↓	88	17	CH ₃ NSC
2091	↓	9	34	
2050	↓	-	8	CH ₃ SNC
2024	↓	18	6	
1930	↑	9	2	
1897	↓	-	3	
1888	↓	-	6	
1735	↓	12	-	HC-CN
1528	↑	29	2	CS ₂
1328	↓	-	34	
1309	↓	12	22	CH ₄
1289	↓	6	59	HS-CH ₂ -NC
1148	↓	-	2	
1123	↓	-	2	
1063	↓	6	-	H ₂ C-CN/CH ₂ =S
996	↓	100	-	CH ₂ =S
993	↓	76	-	CH ₂ =S
936	↓	11	2	HS-CH ₂ -NC
802	↓	-	13	
777	↑	4	6	
723	↓	12	50	
687	↓	29	-	H ₂ C-CN
617	↓	-	3	CH ₃ * tentative detection
483	↓	3	-	HC-CN

1
2
3 A variety of photoproducts were at least tentatively identified, some of which were
4 common across photolysis wavelength and others of which were not. Formation of
5 mercaptoisocyanomethane ($\text{HS-CH}_2\text{-NC}$) was observed at both wavelengths with
6 reasonable certainty and features associated with this species are shown in **Fig 4** with
7 positions listed in **Table 5**. Three peaks were associated with this species whose relative
8 ratio is conserved across multiple experiments, suggesting that they belong to a single
9 photoproduct. While these features are not strong, the agreement of observed line
10 positions and intensities with *ab initio* theoretical results ¹ for $\text{HS-CH}_2\text{-NC}$ (**Table 5**) form
11 a good basis for attribution of these features. The prevalence of CN/NC conversion
12 observed for other cyanide containing carbon chain molecules in a matrix environment
13 also lead us to expect that this transformation will occur.
14
15
16
17
18
19
20
21
22
23
24
25
26
27
28
29

30 **Fig4** Experimental IR spectrum of $\text{HS-CH}_2\text{-NC}$ formed as a photoproduct in an Ar
31 matrix. Y scale is the intensity in arbitrary units.
32

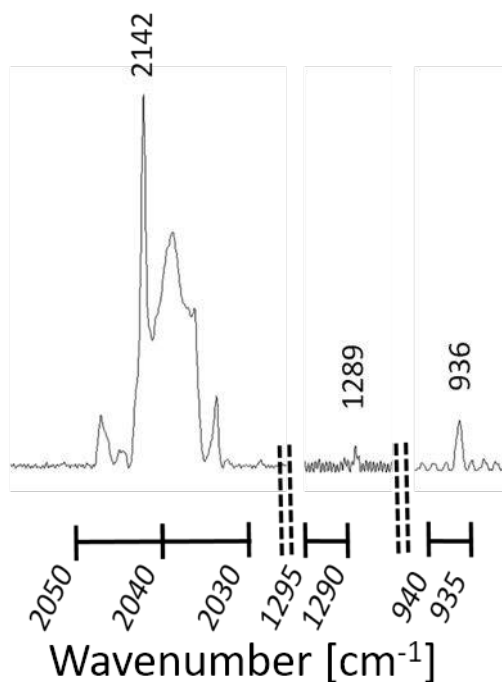


Table 5 Comparison of predicted infrared frequencies and intensities of HS-CH₂-NC with experimental values

Mode	Frequency [cm ⁻¹]		Rel. Int. [unitless]	
	Calc. ^{a)}	Exp.	Calc. ^{b)}	Exp.
v1	2998	-	0	-
v2	2993	-	2	-
v3	2670	-	0	-
v4	2135	2142	100	100
v5	1458	-	4	-
v6	1294	1288.9	15	7
v7	1247	-	4	-
v8	1030	-	1	-
v9	939	935.9	19	12
v10	804	-	1	-
v11	702	-	9	-
v12	416	-	1	-
v13	297	-	3	-
v14	278	-	6	-
v15	171	-	2	-

a) combined CCSD(T)/anharmonic B3LYP calculation, see equation (1) and Ref. 1

b) relative intensities with respect to v4 at 2142 cm⁻¹

Photoisomerization of HS-CH₂-CN into the more stable methyl thiocyanate (CH₃SCN) and methyl isothiocyanate (CH₃NCS) are also likely processes in a matrix environment. Although not presented here, we compared our HS-CH₂-CN photoproduct spectra with those of pure CH₃SCN and CH₃NCS isolated in Ar (work in preparation ⁸⁶). The calculated and measured absolute intensities of IR bands of those two molecules are far larger than for HS-CH₂-CN or HS-CH₂-NC and, as a consequence, even a small amount of CH₃NCS or CH₃SCN formed via photolysis should be easily detectable.

1
2
3 The most stable C_2H_3SN isomer, CH_3NCS , has its most intense vibrations at 2142
4 cm^{-1} and 1419 cm^{-1} with a ratio of 100 to 6⁸⁶. While we were able to distinguish a 2142
5 cm^{-1} vibration, this was assigned to $HS-CH_2-NC$. A band of the parent molecule falls in
6 the exact location of the 1419 cm^{-1} feature. While we cannot rule out the formation of this
7 species, it is impossible to confirm its production here.
8
9

10
11
12 Positive identification of the second isomer, CH_3SCN is also problematic. Peaks
13 located at 2168 cm^{-1} , 1442 cm^{-1} , and 2951 cm^{-1} (with a ratio of intensities of 3:1:1) should
14 be distinguishable⁸⁶. While there is photolytic formation of a species with a vibration at
15 2168 cm^{-1} which might be linked to CH_3SCN , this peak had a very small intensity in all
16 five photolysis experiments performed. The other two vibrations were not observable and
17 may simply have been below the signal-to-noise limit. Stronger evidence is needed to
18 confirm production of CH_3SCN .
19
20
21
22
23
24
25
26
27
28
29

30
31 Some information exists concerning the potential production of the higher energy
32 isomers CH_3CNS and CH_3SNC which were not available commercially or through
33 synthesis. CH_3CNS is likely not formed as the most intense peak, located at 2230 cm^{-1} ⁸⁶,
34 could not be detected.
35
36
37
38
39

40 CH_3SNC has an experimentally assigned vibration at 2050 cm^{-1} accompanied by
41 a smaller feature at 1442 cm^{-1} (intensity ratio of 100:9)⁸⁶. Although a vibration at 2050
42 cm^{-1} is often produced following 193 nm photolysis the second vibration at 1442 cm^{-1} is
43 very close to our limit of detection. Without stronger evidence, CH_3SNC detection cannot
44 be confirmed.
45
46
47
48
49
50

51 The remainder of products observed for this system requires cleavage of at least
52 one bond and separation of the resulting fragments into their own respective matrix cages
53
54
55
56
57
58
59
60

1
2
3 to be produced. For instance, evidence for formation of $\text{H}_2\text{C}=\text{S}$ following 248 nm
4 irradiation suggests that at least some C-C bond cleavage occurs. This photolytic product
5 was identified on the basis of its three most intense bands which were measured
6 previously in an Ar matrix⁵⁸. No $\text{H}_2\text{C}=\text{S}$ was observed following 193 nm irradiation. It may
7 be that the higher photon energy promoted swift loss of the H-atoms from $\text{H}_2\text{C}=\text{S}$ to form
8 CS (followed by CS conversion to CS_2).
9

10
11
12 $\text{H}_2\text{C}-\text{CN}$ and $\text{HC}-\text{CN}$, were likely formed following 248 nm irradiation but not
13 following 193 nm exposure. Both were previously measured in Ar matrix environment,
14 $\text{HC}-\text{CN}$ by Dendramis et al. and by Maier et al.^{87, 88} and $\text{H}_2\text{C}-\text{CN}$ by Cho et al.⁸⁹. $\text{HC}-\text{CN}$
15 was identified in this work as a product on the basis of three unambiguous peaks. For
16 $\text{H}_2\text{C}-\text{CN}$, one peak was unambiguous while a second was very near the limit of detection
17 (not included in table 5). A third peak which should also be visible shares the same
18 location as a band of $\text{H}_2\text{C}=\text{S}$. Overall, detection of $\text{H}_2\text{C}-\text{CN}$ is less certain than $\text{HC}-\text{CN}$.
19
20
21
22
23
24
25
26
27
28
29
30
31
32

33 Formation of both $\text{HC}-\text{CN}$ and $\text{H}_2\text{C}-\text{CN}$ requires cleavage of the S-C bond of $\text{HS}-$
34 CH_2-CN . Given that both $\text{HC}-\text{CN}$ and $\text{H}_2\text{C}-\text{CN}$ were observed, It is reasonable to assume
35 that some HS or H_2S (possibly formed by an escaping HS taking with it another H-atom)
36 might also be detectable. However, based on IR observations of HS and H_2S in an Ar
37 matrix environment⁹⁰, there is no evidence of the formation of either of these in any of
38 the photolyses performed here.. The photochemistry of Ar matrix isolated H_2S and HS
39 have been studied⁹¹⁻⁹³ and H_2S photolysis leads to production of HS followed eventually
40 by atomic sulfur formation. While we have evidence of production of atomic sulfur, from
41 our experiments, described later in discussion of CS_2 formation and annealing, we cannot
42 say whether its production proceeds through H_2S and/or HS, some other intermediate, or
43
44
45
46
47
48
49
50
51
52
53
54
55
56
57
58
59
60

1
2
3 through sequential scission of H atom and then S atom from the H-S-CH₂CN parent.
4

5 A number of other products were also observed at both photolysis wavelengths
6 suggesting that cleavage of single bonds is quite facile and that escape of the fragments
7 thus produced from the matrix cage is also probable. Methane formation, identified here
8 based on comparison with prior measurements in an Ar matrix ⁵⁸, requires cleavage of
9 both S-C and C-C bonds as well as at least one free H atom coming from another matrix
10 site or the possible presence of complexes in a single site. While H atom migration is not
11 a surprising process in a noble gas matrix environment, the formation of CS₂ (identified
12 as compared to measurements in Ar matrix by Szczepanski et al.⁹⁴), possibly from CS
13 and S, requires sulfur atoms coming from two different matrix cages or two parent
14 molecules. This suggests either that free S atoms are somewhat mobile in an Ar matrix,
15 that adjacent matrix sites were near enough to allow minimally mobile S atoms to find one
16 another following photolysis, or a reasonable abundance of HS-CH₂-CN dimers or larger
17 complexes exist in the matrix. Finally, CH₃ identified based on IR measurements in Ar
18 matrix by Pacansky et al. and by Snelson et al. ^{95,96}, was observed upon irradiation at 193
19 nm but not following exposure to 248 nm. Given the presence of CH₄, production of CH₃
20 is logical upon exposure to higher energy photon radiation.
21
22
23
24
25
26
27
28
29
30
31
32
33
34
35
36
37
38
39
40
41

42 Some peaks remain unassigned. Intense peaks, for which we did not find any
43 convincing attribution are marked in the **Table 5**. These lines do not fit with other potential
44 products whose IR signatures in an Ar matrix environment have already been reported:
45 S=CHCN⁹⁷; CH₃CN⁹⁸ or further photolysis products (CH₃NC, CH₂NCH, CH₂CNH,
46 CH₂NC)⁹⁸; CH₃SH⁵⁸; HS⁹⁰; H₂S⁹⁰; CH₂ (NIST gas); HS-CN⁹⁹; or HS-NC⁹⁹.
47
48
49
50
51
52
53

54 We also performed photolysis of Cl-CH₂-CN using 193 nm laser light. As no UV-
55
56
57
58
59
60

1
2
3 VIS spectrum of Cl-CH₂-CN is available in the literature, we measured it and found no
4
5 clear absorption bands between 200 nm and 900 nm, suggesting that two-photon
6
7 processes were involved in photolysis.
8
9

10 The main photolysis product of Cl-CH₂-CN photolysis was Cl-CH₂-NC.

11
12 The position and intensities of peaks of FTIR measurements were compared with
13
14 theoretical calculations and are presented in **Table 2b** and in **Fig5**. The yield of this
15
16 product was high enough that ³⁷Cl isotopomers for ν_6 and ν_7 vibrations could be discerned
17
18 at 775.5 cm⁻¹ and 476.3 cm⁻¹, with intensities proportional to the ratio of natural
19
20 abundances of ³⁵Cl and ³⁷Cl. Additionally, a few small overtone vibrations could be
21
22 distinguished in the spectra ($\nu_6+\nu_3$ at 2208.0 cm⁻¹ and $\nu_{11}+\nu_{10}$ at 2179.0 cm⁻¹). The
23
24 anharmonic computations predicted that both these modes are in resonance with very
25
26 intense ν_2 . It seems that, the intensities of those combinational modes are overestimated,
27
28 but the precise prediction for resonance are far beyond the applied theoretical methods.
29
30 Vibrations at 2144.7 cm⁻¹, 1228.9 cm⁻¹ and 960.6 cm⁻¹ are likely matrix sites of Cl-CH₂-
31
32 NC. Apart from features assigned to the Cl-CH₂-NC product, only six peaks remain
33
34 unassigned (see **Fig 6**): 1982.4 cm⁻¹ (with shoulder centered at 1981.cm⁻¹); 1406.0 cm⁻¹
35
36 (with shoulder centered at 1406.9 cm⁻¹); 1390.4 cm⁻¹, 1387.8 cm⁻¹, 622.8 cm⁻¹ and 617.2
37
38 cm⁻¹. No good evidence for formation of CAN 2 (HNCCCHI) was found (see calculations
39
40
41
42
43
44
45 **Table 2C**).
46
47
48
49
50
51
52
53
54
55
56
57
58
59
60

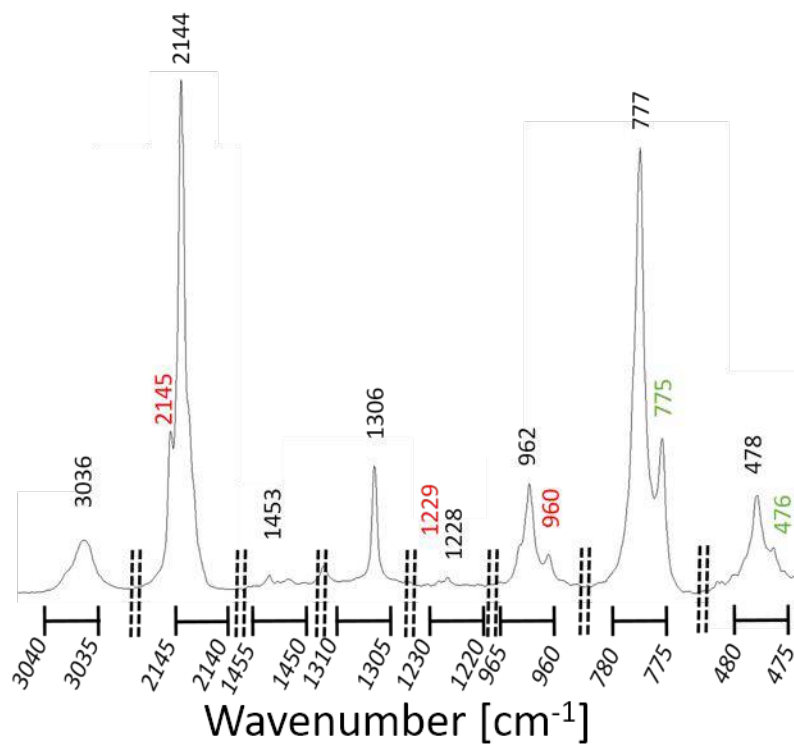
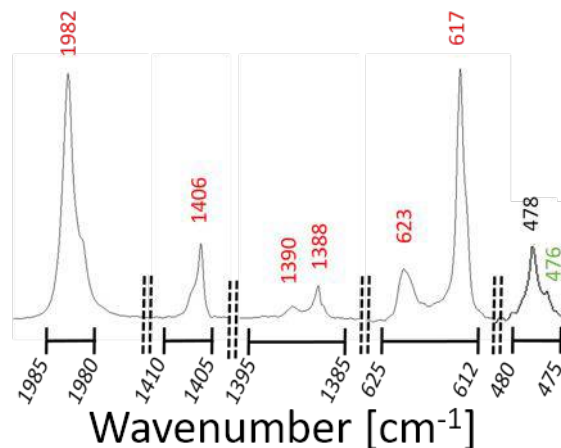


Fig 5 Experimental IR spectrum of Cl-CH₂-NC. Matrix sites assigned to ³⁵Cl-CH₂-CN (black and red) and ³⁷Cl-CH₂-CN (green). Y scale is the intensity in arbitrary units.

* all regions share common x- and y-scales

Fig 6 Unidentified peaks produced during Cl-CH₂-CN photolysis (red labels) along with 475-480cm⁻¹ region (black and green labels) to enable comparison of intensities with **Fig 5**. Y scale is the intensity in arbitrary units.



As S atoms and H atoms seemed to be produced on photolysis of HS-CH₂-CN, it is possible that Cl atom and H atom may be produced upon photolysis of Cl-CH₂-CN. Hydrochloric acid (HCl) is the simplest molecule containing these atoms and, although spectra of Ar matrix isolated HCl are available in the literature, we repeated experiments in a noble gas matrix in the hopes of ruling out HCl or HCl complexes as photoproducts. Our measurements of HCl deposited in Ar matrix match with other published values of the position of the monomer band of HCl in those conditions^{100,101,102,103,104} except for a peak located at 1981.9 cm⁻¹ (compare with **Fig 7**). This is very close to a feature observed following 193 nm photolysis of Cl-CH₂-CN at 1982.4 cm⁻¹, unaccompanied by the main HCl monomer band or bands of any other HCl complex. In terms of HCl measurements, this feature was not present in the gas phase and is not caused by impurities in the HCl sample (samples from different suppliers all exhibited the same feature), noble gas impurities (Ar and Kr both show production of a feature near this location), corrosion of the deposition line (both metal and glass manifolds lead to the same result), or reaction

with deposition window (CsI and sapphire deposition windows also showed the same vibrations). As this peak is not mentioned in the literature either as a band of HCl isolated in a rare gas matrix or as a product of HCl complexation with water or some other species, we take the opportunity to report its presence here.

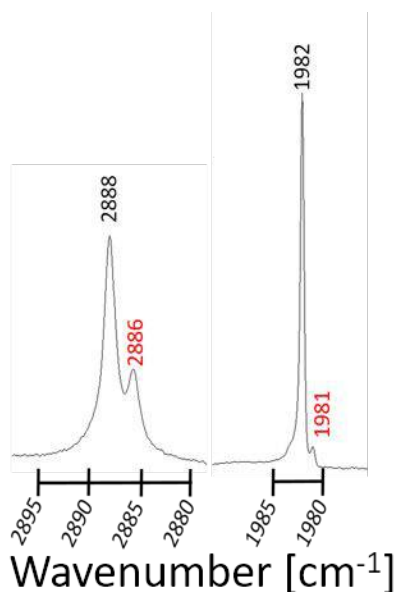


Fig7 Selected regions depicting bands of HCl in an Ar matrix (ratio 1:1000). Red labels are matrix sites. Y scale is the intensity in arbitrary units.

4.4 Annealing

The last step of sample processing was annealing. During annealing, softening of the noble gas matrix can allow some isolated, reactive species to become mobile and recombine, possibly emitting light in the process, and allow changes in specific matrix sites that might be visible in subsequent IR spectra. Aside from confirming photoproduct assignment using IR spectra, we also monitored for light emission during annealing using a low resolution CCD spectrometer. Following 193 nm irradiation of HS-CH₂-CN, three different emission signals were observed, one starting at around 8 K, a second between 8 and 12 K, and a third above 12 K. Just above 8K, we were able to see a greenish glow (a broad weak line at 521 nm) (**Fig8**).

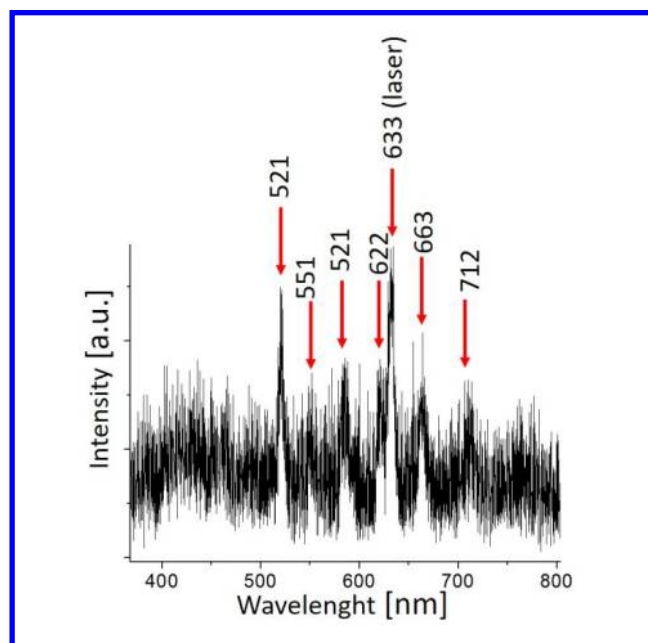


Fig8 Glow after photolysis of HS-CH₂-CN at 10K

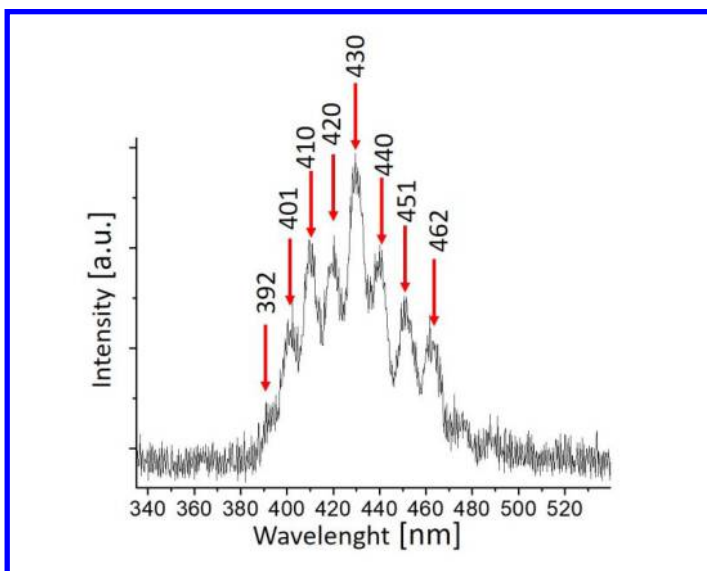


Fig9 Glow after photolysis of HS-CH₂-CN at 20 K assigned to OCS

Although we do not have any explanation for this emission, annealing of the photolysed sample of Cl-CH₂-CN also produced this greenish glow which allows us to conclude that it is not related to the presence of sulfur. When heating photolysed samples of HS-CH₂-CN between 8K and 10K, additional glows at 551, 586 nm, 622 nm, 663 nm and 712.5 nm (**Fig8**) appeared. We attribute this progression to SO ($c\ ^1\Sigma^- \rightarrow a\ ^1\Delta$) emission¹⁰⁵.

1
2
3 Excited SO is produced through the reaction between ground state S(3P_2) and O(3P_2)
4 atoms where the main source of atomic oxygen in our sample may be photolysis of CO₂
5 into CO and O. Above 12 K, a large amount of sulfur (3P) was mobilized¹⁰⁶.
6
7
8
9
10 Recombination with CO($X^1\Sigma^+$) forms electronically excited OCS and produces a bluish
11
12
13
14
15
16
17
18
19
20
21
22
23
24
25
26
27
28
29
30
31
32
33
34
35
36
37
38
39
40
41
42
43
44
45
46
47
48
49
50
51
52
53
54
55
56
57
58
59
60
afterglow with vibrational spacing of around 550 cm⁻¹ and maximum at 430 nm (see **Fig 9**). The glow persists up to 25 K. The temperature separation of SO and OCS emission is likely a consequence of the larger mobility of atomic oxygen compared with sulfur in an Ar matrix which allows it to become mobile at a lower temperature.

5. Conclusions

We have investigated the photochemistry of mercaptoacetonitrile (HS-CH₂-CN) and chloroacetonitrile (Cl-CH₂-CN) in noble gas (Ar) matrices at 6K. We determined position and intensities of peaks and supported our conclusions with computational analysis. For both, isocyanide compounds (HS-CH₂-NC and Cl-CH₂-NC) were identified. While no products indicating ejection of Cl or other moieties from the matrix cage were identified for Cl-CH₂-CN, evidence exists for a variety of processes in the case of HS-CH₂-CN. For example, production of CS₂ following photolysis and observation of emission by SO and OCS upon subsequent annealing suggest formation of a mobilized free sulfur atom upon photolysis of HS-CH₂-CN. Observation of CH₂-CN and CH-CN show loss of HS. The formation of CH₂=S indicate the loss of CN while production of CH₄ provide evidence for the loss of both HS and CN.

1
2
3
4
5
6
7
8
9
10
11
12
13
14
15
16
17
18
19
20
21
22
23
24
25
26
27
28
29
30
31
32
33
34
35
36
37
38
39
40
41
42
43
44
45
46
47
48
49
50
51
52
53
54
55
56
57
58
59
60

Supporting information

Tables with comparison of results of this work with previous reports for HSCH₂CN and for ClCH₂CN

Acknowledgments

This work was supported by NCN grant 2015/17/B/ST4/03875.

J.-C. G. thanks the Centre National d'Etudes Spatiales (CNES) and the French Programme National "Physique et Chimie du Milieu Interstellaire" for financial support.

Reference list:

1. Gronowski, M.; Turowski, M.; Custer, T.; Kołos, R., A Theoretical Study on the Spectroscopy, Structure, and Stability of C₂H₃NS Molecules. *Theoretical Chemistry Accounts* **2016**, *135* (9), 222.
2. Gibb, E.; Nummelin, A.; Irvine, W. M.; Whittet, D. C. B.; Bergman, P., Chemistry of the Organic-Rich Hot Core G327.3–0.6. *The Astrophysical Journal* **2000**, *545* (1), 309.
3. Frerking, M.; Linke, R.; Thaddeus, P., *Interstellar isothiocyanic acid*. 1980; Vol. 234.
4. Halfen, D. T.; Ziurys, L. M.; Brünken, S.; Gottlieb, C. A.; McCarthy, M. C.; Thaddeus, P., Detection of a New Interstellar Molecule: Thiocyanic Acid HSCN. *The Astrophysical Journal Letters* **2009**, *702* (2), L124.
5. Nayak, M. K.; Chaudhuri, R. K.; Krishnamachari, S. N. L. G., Theoretical study on the excited states of HCN. *The Journal of Chemical Physics* **2005**, *122* (18), 184323.
6. Thiel, V.; Belloche, A.; Menten, K. M.; Garrod, R. T.; Müller, H. S. P., Complex organic molecules in diffuse clouds along the line of sight to Sagittarius B2. *Astronomy & Astrophysics* **2017**, *605*.
7. Danger, G.; Rimola, A.; Abou Mrad, N.; Duvernay, F.; Roussin, G.; Theule, P.; Chiavassa, T., Formation of hydroxyacetonitrile (HOCH₂CN) and polyoxymethylene (POM)-derivatives in comets from formaldehyde (CH₂O) and hydrogen cyanide (HCN) activated by water. *Physical Chemistry Chemical Physics* **2014**, *16* (8), 3360-3370.
8. Zeng, S.; Quénard, D.; Jiménez-Serra, I.; Martín-Pintado, J.; Rivilla, V. M.; Testi, L.; Martín-Doménech, R., First detection of the pre-biotic molecule glycolonitrile (HOCH₂CN) in the interstellar medium. *Monthly Notices of the Royal Astronomical Society: Letters* **2019**, *484* (1), L43-L48.
9. Wakelam, V.; Hersant, F.; Herpin, F., Sulfur Chemistry: 1d Modeling in Massive Dense Cores. *Astronomy & Astrophysics* **2011**, *529*, A112.
10. Liu, H. B.; Jiménez-Serra, I.; Ho, P. T. P.; Chen, H.-R.; Zhang, Q.; Li, Z.-Y., Fragmentation and Ob Star Formation in High-Mass Molecular Hub-Filament Systems. *The Astrophysical Journal* **2012**, *756* (1), 10.
11. Li, J.; Wang, J.; Zhu, Q.; Zhang, J.; Li, D., Sulfur-Bearing Molecules in Massive Star-Forming Regions: Observations of Ocs, Cs, H₂s, and So. *The Astrophysical Journal* **2015**, *802* (1), 40.
12. Esplugues, G. B.; Viti, S.; Goicoechea, J. R.; Cernicharo, J., Modelling the Sulphur Chemistry Evolution in Orion KL. *Astronomy & Astrophysics* **2014**, *567*, A95.
13. Woods, P. M.; Occhiogrosso, A.; Viti, S.; Ka uchova, Z.; Palumbo, M. E.; Price, S. D., A New Study of an Old Sink of Sulphur in Hot Molecular Cores: The Sulphur Residue. *Monthly Notices of the Royal Astronomical Society* **2015**, *450* (2), 1256-1267.
14. Linke, R. A.; Frerking, M. A.; Thaddeus, P., Interstellar Methyl Mercaptan. *The Astrophysical Journal* **1979**, *234*, L139.
15. Gibb, E.; Nummelin, A.; Irvine, W. M.; Whittet, D. C. B.; Bergman, P., Chemistry of the Organic-Rich Hot Core G327.3–0.6. *The Astrophysical Journal* **2000**, *545* (1), 309-326.
16. Wakelam, V.; Loison, J. C.; Herbst, E.; Pavone, B.; Bergeat, A.; Béroff, K.; Chabot, M.; Faure, A.; Galli, D.; Geppert, W. D.; Gerlich, D.; Gratier, P.; Harada, N.; Hickson, K. M.; Honvault, P.; Klippenstein, S. J.; Picard, S. D. L.; Nyman, G.; Ruaud, M.; Schlemmer, S.; Sims, I. R.; Talbi, D.; Tennyson, J.; Wester, R., The 2014 KIDA Network for Interstellar Chemistry. *The Astrophysical Journal Supplement Series* **2015**, *217* (2), 20.
17. Goicoechea, J. R.; Pety, J.; Gerin, M.; Teyssier, D.; Roueff, E.; Hily-Blant, P.; Baek, S., Low Sulfur Depletion in the Horsehead Pdr. *Astronomy and Astrophysics* **2006**, *456* (2), 565-580.
18. Fayolle, E. C.; Öberg, K. I.; Jørgensen, J. K.; Altwegg, K.; Calcutt, H.; Müller, H. S. P.; Rubin, M.; van der Wiel, M. H. D.; Bjerkeli, P.; Bourke, T. L.; Coutens, A.; van Dishoeck, E. F.; Drozdovskaya, M. N.; Garrod, R. T.; Ligterink, N. F. W.; Persson, M. V.; Wampfler, S. F.; Balsiger,

H.; Berthelier, J. J.; De Keyser, J.; Fiethe, B.; Fuselier, S. A.; Gasc, S.; Gombosi, T. I.; Sémon, T.; Tzou, C. Y.; the, R. t., Protostellar and cometary detections of organohalogens. *Nature Astronomy* **2017**, *1* (10), 703-708.

19. Öberg, K. I., Photochemistry and Astrochemistry: Photochemical Pathways to Interstellar Complex Organic Molecules. *Chemical Reviews* **2016**, *116* (17), 9631-9663.

20. d'Hendecourt, L.; Dartois, E., Interstellar matrices: the chemical composition and evolution of interstellar ices as observed by ISO. *Spectrochimica Acta Part A: Molecular and Biomolecular Spectroscopy* **2001**, *57* (4), 669-684.

21. Møllendal, H.; Samdal, S.; Guillemin, J.-C., Rotational Spectrum, Conformational Composition, Intramolecular Hydrogen Bonding, and Quantum Chemical Calculations of Mercaptoacetonitrile (HSCH₂C≡N), a Compound of Potential Astrochemical Interest. *The Journal of Physical Chemistry A* **2016**, *120* (12), 1992-2001.

22. Bacchus-Montabonel, M.-C., Proton-induced collision dynamics on potential prebiotic sulfur species. *Physical Chemistry Chemical Physics* **2018**, *20* (14), 9084-9089.

23. Mathias, E.; Shimanski, M., Synthesis of mercaptoacetonitrile under mild conditions. *Journal of the Chemical Society, Chemical Communications* **1981**, (11), 569-570.

24. Wepplo, P., Synthesis of Mercaptoacetonitrile and Cyanomethyl Thioesters. *Synthetic Communications* **1989**, *19* (9-10), 1533-1538.

25. Gaumont, A. C.; Wazneh, L.; Denis, J. M., Thiocyanohydrins, a New Class of Compounds, Precursors of Unstabilized Thiocarbonyl Derivatives. *Tetrahedron* **1991**, *47* (27), 4927-4940.

26. Alexander, S. R.; Fairbanks, A. J., Direct aqueous synthesis of cyanomethyl thioglycosides from reducing sugars; ready access to reagents for protein glycosylation. *Organic & Biomolecular Chemistry* **2016**, *14* (28), 6679-6682.

27. Zeil, v. W., Die Schwingungsspektren der chlorierten Acetonitrile. In *Zeitschrift für Physikalische Chemie*, 1958; Vol. 14, p 230.

28. Durig, J. R.; Wertz, D. W., Far infrared and Raman spectra of the haloacetonitriles. *Spectrochimica Acta Part A: Molecular Spectroscopy* **1968**, *24* (1), 21-29.

29. Jones, R. G.; Orville-Thomas, W. J., 862. Spectroscopic studies. Part V. The spectra and structure of monohalogenoacetonitriles. *Journal of the Chemical Society (Resumed)* **1965**, (0), 4632-4646.

30. van Der Kelen, G. P., Studies on Halogenated Aliphatic Compounds VII. Dipole Moments and Infrared Spectra of Halogenated Acetonitriles. *Bulletin des Sociétés Chimiques Belges* **1962**, *71* (7-8), 421-430.

31. Allerhand, A.; von Rague Schleyer, P., Nitriles and Isonitriles as Proton Acceptors in Hydrogen Bonding: Correlation of $\Delta\nu_{OH}$ with Acceptor Structure. *Journal of the American Chemical Society* **1963**, *85* (7), 866-870.

32. Schumann, H.; Speis, M.; Bosman, W. P.; Smits, J. M. M.; Beurskens, P. T., Monosubstituted nitrogen donors as ligands in cyclopentadienyliron complexes: synthesis, reactivity, ligand properties, and crystal structure of [C₅H₅Fe(CO)₂(C₅H₅N)]SbF₆. *Journal of Organometallic Chemistry* **1991**, *403* (1), 165-182.

33. Augdahl, E.; Klaboe, P., Spectroscopic studies of charge transfer complexes—VI: Nitriles and iodine monochloride. *Spectrochimica Acta* **1963**, *19* (10), 1665-1673.

34. Butt, G.; Cilmi, J.; Hoobin, P. M.; Topsom, R. D., The transmission of resonance effects through a methylene group—spectroscopic studies on some α -substituted-acetonitriles and p-toluenitriles. *Spectrochimica Acta Part A: Molecular Spectroscopy* **1980**, *36* (6), 521-524.

35. Crowder, G. A., Force constants and normal vibrations of the haloacetonitriles. *Molecular Physics* **1972**, *23* (4), 707-715.

36. Wladkowski, B. D.; Lim, K. F.; Allen, W. D.; Brauman, J. I., The S_N2 identity exchange reaction ClCH₂CN + Cl⁻. f.wdarw. Cl⁻ + ClCH₂CN: experiment and theory. *Journal of the American Chemical Society* **1992**, *114* (23), 9136-9153.

37. Nemes, L.; Orville-Thomas, W. J., Infra-red dispersion studies. Part 3.—Band intensities

- of acetonitrile and its chlorinated derivatives. *Transactions of the Faraday Society* **1965**, *61* (0), 1839-1849.
38. Nemes, L.; Orville-Thomas, W. J., Infra-red dispersion studies. Part 5.—Variation of intensity with change of phase for acetonitrile and its chlorinated derivatives. *Transactions of the Faraday Society* **1965**, *61* (0), 2612-2622.
39. Thomas, B. H.; Orville-Thomas, W. J., Infrared intensities of $V(C\equiv N)$ bands. *Journal of Molecular Structure* **1971**, *7* (1), 123-135.
40. George, W. O.; Hirani, P. K.; Lewis, E. N.; Maddams, W. F.; Williams, D. A., Aggregation and association of polar molecules in low temperature matrices and in the gaseous phase. *Journal of Molecular Structure* **1986**, *141*, 227-236.
41. Apkarian, V. A.; Schwentner, N., Molecular Photodynamics in Rare Gas Solids. *Chemical Reviews* **1999**, *99* (6), 1481-1514.
42. E. Bondybey, V.; Räsänen, M.; Lammers, A., Chapter 10. Rare-gas matrices, their photochemistry and dynamics: recent advances in selected areas. *Annual Reports Section "C" (Physical Chemistry)* **1999**, *95* (0), 331-372.
43. Kołos, R.; Sobolewski, A. L., The Infrared Spectroscopy of Hnccc: Matrix Isolation and Density Functional Theory Study. *Chemical Physics Letters* **2001**, *344* (5-6), 625-630.
44. Kawaguchi, K.; Ohishi, M.; Ishikawa, S.-I.; Kaifu, N., Detection of Isocyanoacetylene HCCNC in TMC-1. *The Astrophysical Journal* **1992**, *386*, L51-L53.
45. Kawaguchi, K.; Takano, S.; Ohishi, M.; Ishikawa, S.-I.; Miyazawa, K.; Kaifu, N.; Yamashita, K.; Yamamoto, S.; Saito, S.; Ohshima, Y.; Endo, Y., Detection of HNCCC in TMC-1. *The Astrophysical Journal* **1992**, *396*, L49-L51.
46. Gensheimer, P. D., Observations of HCCNC and HNCCC in IRC+10216. *Astrophysics and Space Science* **1997**, *251* (1), 199-202.
47. Vastel, C.; Kawaguchi, K.; Quénard, D.; Ohishi, M.; Lefloch, B.; Bachiller, R.; Müller, H. S. P., High spectral resolution observations of HNC3 and HCCNC in the L1544 pre-stellar core. *Monthly Notices of the Royal Astronomical Society: Letters* **2018**, *474* (1), L76-L80.
48. Coupeaud, A.; Turowski, M.; Gronowski, M.; Pietri, N.; Couturier-Tamburelli, I.; Kołos, R.; Aycard, J. P., Spectroscopy of Cyanodiacetylene in Solid Argon and the Photochemical Generation of Isocyanodiacetylene. *Journal of Chemical Physics* **2007**, *126* (16), 164301.
49. Smith, A. M.; Schallmoser, G.; Thoma, A.; Bondybey, V. E., Infrared spectral evidence of $N\equiv C-C\equiv C-N\equiv C$: Photoisomerization of $N\equiv C-C\equiv C-C\equiv N$ in an argon matrix. *The Journal of Chemical Physics* **1993**, *98* (3), 1776-1785.
50. Kołos, R., Photolysis of dicyanodiacetylene in argon matrices. *Chemical Physics Letters* **1999**, *299* (2), 247-251.
51. Kołos, R.; Waluk, J., Matrix-Isolated Products of Cyanoacetylene Dissociation. *Journal of Molecular Structure* **1997**, *408-409*, 473-476.
52. Callear, A. B.; Dickson, D. R., Transient spectra and primary processes in the flash photolysis of CH_3SSCH_3 , CH_3SCH_3 , CH_3SH and C_2H_5SH . *Transactions of the Faraday Society* **1970**, *66* (0), 1987-1995.
53. Bridges, L.; White, J. M., Photochemistry of methanethiol at 254 and 214 nm. *The Journal of Physical Chemistry* **1973**, *77* (2), 295-298.
54. Jensen, E.; Keller, J. S.; Waschewsky, G. C. G.; Stevens, J. E.; Graham, R. L.; Freed, K. F.; Butler, L. J., Dissociation dynamics of CH_3SH at 222, 248, and 193 nm: An analog for probing nonadiabaticity in the transition state region of bimolecular reactions. *The Journal of Chemical Physics* **1993**, *98* (4), 2882-2890.
55. Skelton, J.; Adam, F. C., The Photolysis and Radiolysis of Simple Mercaptans in Dilute Glassy Matrices. *Canadian Journal of Chemistry* **1971**, *49* (21), 3536-3543.
56. Bridges, L.; Hemphill, G. L.; White, J. M., Photochemistry of ethanethiol at 254 and 214 nm. *The Journal of Physical Chemistry* **1972**, *76* (19), 2668-2673.
57. Steer, R. P.; Knight, A. R., Reactions of thiyl radicals. VI. Photolysis of ethanethiol.

1
2
3 *Canadian Journal of Chemistry* **1969**, *47* (8), 1335-1345.

4 58. Jacox, M. E.; Milligan, D. E., Matrix isolation study of the infrared spectrum of
5 thioformaldehyde. *Journal of Molecular Spectroscopy* **1975**, *58* (1), 142-157.

6 59. Jacox, M. E.; Milligan, D. E., Matrix-Isolation Study of the Vacuum-Ultraviolet Photolysis
7 of Methyl Fluoride. The Infrared Spectra of the Free Radicals CF, HCF, and H₂CF. *The Journal*
8 *of Chemical Physics* **1969**, *50* (8), 3252-3262.

9 60. Jacox, M. E.; Milligan, D. E., Matrix-Isolation Study of the Vacuum-Ultraviolet Photolysis
10 of Methyl Chloride and Methylene Chloride. Infrared and Ultraviolet Spectra of the Free Radicals
11 CCl, H₂CCl, and CCl₂. *The Journal of Chemical Physics* **1970**, *53* (7), 2688-2701.

12 61. Becke, A. D., Density-Functional Thermochemistry. III. The Role of Exact Exchange. *The*
13 *Journal of Chemical Physics* **1993**, *98* (7), 5648-5652.

14 62. Lee, C.; Yang, W.; Parr, R. G., Development of the Colle-Salvetti correlation-energy
15 formula into a functional of the electron density. *Physical Review B* **1988**, *37* (2), 785-789.

16 63. Cossi, M.; Rega, N.; Scalmani, G.; Barone, V., Energies, structures, and electronic
17 properties of molecules in solution with the C-PCM solvation model. *Journal of Computational*
18 *Chemistry* **2003**, *24* (6), 669-681.

19 64. Barone, V., Vibrational zero-point energies and thermodynamic functions beyond the
20 harmonic approximation. *The Journal of Chemical Physics* **2004**, *120* (7), 3059-3065.

21 65. Barone, V., Anharmonic vibrational properties by a fully automated second-order
22 perturbative approach. *The Journal of Chemical Physics* **2004**, *122* (1), 014108.

23 66. Bloino, J.; Barone, V., A second-order perturbation theory route to vibrational averages
24 and transition properties of molecules: General formulation and application to infrared and
25 vibrational circular dichroism spectroscopies. *The Journal of Chemical Physics* **2012**, *136* (12),
26 124108.

27 67. Bartlett, R. J.; Purvis, G. D., Many-body perturbation theory, coupled-pair many-electron
28 theory, and the importance of quadruple excitations for the correlation problem. *International*
29 *Journal of Quantum Chemistry* **1978**, *14* (5), 561-581.

30 68. Pople, J. A.; Krishnan, R.; Schlegel, H. B.; Binkley, J. S., Electron correlation theories and
31 their application to the study of simple reaction potential surfaces. *International Journal of*
32 *Quantum Chemistry* **1978**, *14* (5), 545-560.

33 69. Purvis, G. D.; Bartlett, R. J., A full coupled-cluster singles and doubles model: The
34 inclusion of disconnected triples. *The Journal of Chemical Physics* **1982**, *76* (4), 1910-1918.

35 70. Scuseria, G. E.; Janssen, C. L.; Schaefer, H. F., An efficient reformulation of the
36 closed-shell coupled cluster single and double excitation (CCSD) equations. *The Journal of*
37 *Chemical Physics* **1988**, *89* (12), 7382-7387.

38 71. Pople, J. A.; Head-Gordon, M.; Raghavachari, K., Quadratic configuration interaction. A
39 general technique for determining electron correlation energies. *The Journal of Chemical Physics*
40 **1987**, *87* (10), 5968-5975.

41 72. Dunning, T. H., Gaussian Basis Sets for Use in Correlated Molecular Calculations. I. The
42 Atoms Boron through Neon and Hydrogen. *The Journal of Chemical Physics* **1989**, *90* (2), 1007.

43 73. Kendall, R. A.; Dunning, T. H.; Harrison, R. J., Electron Affinities of the First-Row Atoms
44 Revisited. Systematic Basis Sets and Wave Functions. *The Journal of Chemical Physics* **1992**,
45 *96* (9), 6796.

46 74. Frisch, M. J.; Trucks, G. W.; Schlegel, H. B.; Scuseria, G. E.; Robb, M. A.; Cheeseman,
47 J. R.; Scalmani, G.; Barone, V.; Mennucci, B.; Petersson, G. A.; Nakatsuji, H.; Caricato, M.; Li,
48 X.; Hratchian, H. P.; Izmaylov, A. F.; Bloino, J.; Zheng, G.; Sonnenberg, J. L.; Hada, M.; Ehara,
49 M.; Toyota, K.; Fukuda, R.; Hasegawa, J.; Ishida, M.; Nakajima, T.; Honda, Y.; Kitao, O.; Nakai,
50 H.; Vreven, T.; Montgomery Jr., J. A.; Peralta, J. E.; Ogliaro, F.; Bearpark, M. J.; Heyd, J.;
51 Brothers, E. N.; Kudin, K. N.; Staroverov, V. N.; Kobayashi, R.; Normand, J.; Raghavachari, K.;
52 Rendell, A. P.; Burant, J. C.; Iyengar, S. S.; Tomasi, J.; Cossi, M.; Rega, N.; Millam, N. J.; Klene,
53 M.; Knox, J. E.; Cross, J. B.; Bakken, V.; Adamo, C.; Jaramillo, J.; Gomperts, R.; Stratmann, R.

- 1
2
3 E.; Yazyev, O.; Austin, A. J.; Cammi, R.; Pomelli, C.; Ochterski, J. W.; Martin, R. L.; Morokuma,
4 K.; Zakrzewski, V. G.; Voth, G. A.; Salvador, P.; Dannenberg, J. J.; Dapprich, S.; Daniels, A. D.;
5 Farkas, A. d.; Foresman, J. B.; Ortiz, J. V.; Cioslowski, J.; Fox, D. J. *Gaussian 09*, Gaussian, Inc.:
6 Wallingford, CT, USA, 2009.
- 7 75. Puzzarini, C.; Biczysko, M.; Barone, V., Accurate Harmonic/Anharmonic Vibrational
8 Frequencies for Open-Shell Systems: Performances of the B3LYP/N07D Model for Semirigid
9 Free Radicals Benchmarked by CCSD(T) Computations. *Journal of Chemical Theory and
10 Computation* **2010**, *6* (3), 828-838.
- 11 76. Coupeaud, A.; Turowski, M.; Gronowski, M.; Piétri, N.; Couturier-Tamburelli, I.; Kołos, R.;
12 Aycard, J.-P., C5N⁻ anion and new carbenic isomers of cyanodiacetylene: A matrix isolation IR
13 study. *The Journal of Chemical Physics* **2008**, *128* (15), 154303.
- 14 77. Kołos, R.; Gronowski, M.; Dobrowolski, J. C., Prospects for the Detection of Interstellar
15 Cyanovinylidene. *The Astrophysical Journal* **2009**, *701* (1), 488.
- 16 78. Gronowski, M. Teoria I Eksperyment W Badaniach Spektroskopii Wybranych Nityli O
17 Znaczeniu Astrochemicznym Oraz Czasteczek Pokrewnych. PhD Thesis, Institute of Physical
18 Chemistry Polish Academy of Sciences, Poland, Warszawa, 2010.
- 19 79. Szczepaniak, K.; Person, W. B., Measurement of the absolute infrared intensity of the
20 fundamental vibration of HCl in low temperature matrices. *Journal of Molecular Structure* **1982**,
21 *80*, 309-316.
- 22 80. Urso, R. G.; Scirè, C.; Baratta, G. A.; Compagnini, G.; Palumbo, M. E., Combined infrared
23 and Raman study of solid CO. *Astronomy & Astrophysics* **2016**, *594*.
- 24 81. Seidel, G. M.; Lanou, R. E.; Yao, W. In *Rayleigh scattering in rare-gas liquids*, 2002.
- 25 82. Kisiel, Z.; Pszczolkowski, L., The Millimeter-Wave Rotational Spectrum of
26 Chloroacetonitrile. *Journal of Molecular Spectroscopy* **1993**, *158* (2), 318-327.
- 27 83. Mollendal, H.; Samdal, S.; Guillemin, J. C., Rotational Spectrum, Conformational
28 Composition, Intramolecular Hydrogen Bonding, and Quantum Chemical Calculations of
29 Mercaptoacetonitrile (HSCH₂CN), a Compound of Potential Astrochemical Interest. *J Phys Chem
30 A* **2016**, *120* (12), 1992-2001.
- 31 84. Dobrowolski, J. C.; Jamróz, M. H.; Kołos, R.; Rode, J. E.; Cyrański, M. K.; Sadlej, J., IR
32 low-temperature matrix, X-ray and ab initio study on l-isoserine conformations. *Physical
33 Chemistry Chemical Physics* **2010**, *12* (36), 10818-10830.
- 34 85. Dobrowolski, J. C.; Jamróz, M. H.; Kołos, R.; Rode, J. E.; Sadlej, J., IR Low-Temperature
35 Matrix and ab Initio Study on β-Alanine Conformers. *ChemPhysChem* **2008**, *9* (14), 2042-2051.
- 36 86. Turowski, M.; Gronowski, M.; Custer, T.; Zapala, J.; Guillemin, J. C.; Kołos, R.,
37 Isomerization of methyl isothiocyanate and methyl thiocyanate in argon matrices induced by UV
38 irradiation. in preparation.
- 39 87. Dendramis, A.; Leroi, G. E., Matrix isolation spectroscopic study of the free radical HCCN.
40 *The Journal of Chemical Physics* **1977**, *66* (10), 4334-4340.
- 41 88. Maier, G.; Reisenauer, H. P.; Rademacher, K., Cyanocarbene, Isocyanocarbene, and
42 Azacyclopropenylidene: A Matrix-Spectroscopic Study. *Chemistry – A European Journal* **1998**, *4*
43 (10), 1957-1963.
- 44 89. Cho, H.-G.; Andrews, L., Matrix Infrared Spectra and Density Functional Calculations of
45 the H₂CCN and H₂CNC Radicals Produced from CH₃CN. *The Journal of Physical Chemistry A*
46 **2011**, *115* (31), 8638-8642.
- 47 90. Isoniemi, E.; Pettersson, M.; Khriachtchev, L.; Lundell, J.; Räsänen, M., Infrared
48 Spectroscopy of H₂S and SH in Rare-Gas Matrixes. *The Journal of Physical Chemistry A* **1999**,
49 *103* (6), 679-685.
- 50 91. Koda, S.; Koga, K.; Takizawa, K.; Ihara, Y.; Takami, A., *Photodissociation of H₂S doped
51 in low temperature rare gas solids under UV irradiation*. 2001; Vol. 274, p 283-289.
- 52 92. Continetti, R.; Balko, B.; Lee, Y. T., *Photodissociation of H₂S and the HS radical at 193.3
53 nm*. 1991; Vol. 182, p 400-405.
- 54
55
56
57
58
59
60

- 1
2
3 93. Khriachtchev, L.; Pettersson, M.; Isoniemi, E.; Räsänen, M., 193 nm photolysis of H₂S in
4 rare-gas matrices: Luminescence spectroscopy of the products. *The Journal of Chemical Physics*
5 **1998**, *108* (14), 5747-5754.
- 6 94. Szczepanski, J.; Hodyss, R.; Fuller, J.; Vala, M., Infrared Absorption Spectroscopy of
7 Small Carbon-Sulfur Clusters Isolated in Solid Ar. *The Journal of Physical Chemistry A* **1999**, *103*
8 (16), 2975-2981.
- 9 95. Pacansky, J.; Bargon, J., Low temperature photochemical studies on acetyl benzoyl
10 peroxide. Observation of methyl and phenyl radicals by matrix isolation infrared spectroscopy.
11 *Journal of the American Chemical Society* **1975**, *97* (23), 6896-6897.
- 12 96. Snelson, A., Infrared matrix isolation spectrum of the methyl radical produced by pyrolysis
13 of methyl iodide and dimethyl mercury. *The Journal of Physical Chemistry* **1970**, *74* (3), 537-544.
- 14 97. Kappe, C. O.; Wah Wong, M.; Wentrup, C., Matrix isolation and infrared spectrum of
15 thioformyl cyanide. *Tetrahedron Letters* **1993**, *34* (41), 6623-6626.
- 16 98. Kameneva, S. V.; Volosatova, A. D.; Feldman, V. I., Radiation-induced transformations of
17 isolated CH₃CN molecules in noble gas matrices. *Radiation Physics and Chemistry* **2017**, *141*,
18 363-368.
- 19 99. Wierzejewska, M.; Mielke, Z., Photolysis of isothiocyanic acid HNCS in low-temperature
20 matrices. Infrared detection of HSCN and HSNC isomers. *Chemical Physics Letters* **2001**, *349*
21 (3), 227-234.
- 22 100. Anderson, D. T.; Davis, S.; Nesbitt, D. J., Sequential solvation of HCl in argon: High
23 resolution infrared spectroscopy of Ar_nHCl (n=1,2,3). *The Journal of Chemical Physics* **1997**, *107*
24 (4), 1115-1127.
- 25 101. Kalinowski, J.; Gerber, R. B.; Räsänen, M.; Lignell, A.; Khriachtchev, L., Matrix effect on
26 vibrational frequencies: Experiments and simulations for HCl and HNgCl (Ng = Kr and Xe). *The*
27 *Journal of Chemical Physics* **2014**, *140* (9), 094303.
- 28 102. Lorenz, M.; Kraus, D.; Räsänen, M.; Bondybey, V. E., Photodissociation of hydrogen
29 halides in rare gas matrices, and the effect of hydrogen bonding. *The Journal of Chemical Physics*
30 **2000**, *112* (8), 3803-3811.
- 31 103. Howard, B. J.; Pine, A. S., Rotational predissociation and libration in the infrared spectrum
32 of Ar□HCl. *Chemical Physics Letters* **1985**, *122* (1), 1-8.
- 33 104. Boulet, C.; Flaud, P. M.; Hartmann, J. M., Infrared line collisional parameters of HCl in
34 argon, beyond the impact approximation: Measurements and classical path calculations. *The*
35 *Journal of Chemical Physics* **2004**, *120* (23), 11053-11061.
- 36 105. Lee, Y. P.; Pimentel, G. C., Chemiluminescence of S₂ in solid argon. *The Journal of*
37 *Chemical Physics* **1979**, *70* (2), 692-698.
- 38 106. Brom, J. M.; Lepak, E. J., Afterglow from the photodissociation OCS in an argon matrix at
39 4K. *Chemical Physics Letters* **1976**, *41* (1), 185-187.
- 40
41
42
43
44
45
46
47
48
49
50
51
52
53
54
55
56
57
58
59
60

